Theory of Deep-Inelastic Lepton-Nucleon Scattering and Lepton-Pair Annihilation Processes.* III. Deep-Inelastic Electron-Positron Annihilation

SIDNEY D. DRELL, DONALD J. LEVY, AND TUNG-MOW YAN
Stanford Linear Accelerator Center, Stanford University, Stanford, California 94305

(Received 30 October 1969)

This is the third in a series of four papers devoted to a theoretical study based on canonical quantum field theory of the deep-inelastic lepton processes. In the present paper we present the detailed calculations leading to the limiting behavior—or the "parton model"—for deep-inelastic electron-positron annihilation into a nucleon (or hadron) plus "anything else," i.e., $e^-+e^+ \to p+$"anything," where "anything" refers to all possible hadrons. In particular, we show that the structure functions satisfy a scaling behavior analogous to the Bjorken limit for deep-inelastic scattering. The precise relation of the structure functions for deep-inelastic annihilation processes to those for the deep-inelastic scattering is discussed along with specific experimental implications and tests.

I. INTRODUCTION

THIS is the third in a series of four papers on lepton-hadron interactions[1] and focuses on the study of the annihilation of electron-positron pairs into a nucleon plus "anything else" in the deep inelastic region.

In such processes one measures the matrix elements of the hadronic electromagnetic current operator in kinematic regions entirely different from those available in the scattering experiments. The two processes, annihilation and scattering, are nevertheless related by the crossing properties of field theory or equivalently of Feynman graphs. It is therefore of great interest to study precisely what we can infer from deep-inelastic electron-nucleon scattering about deep-inelastic electron-positron annihilation to a nucleon plus "anything else."

In particular, we are interested in finding out if there is an analog in this case to the Bjorken limit and to the scaling behavior for the structure functions as found in the deep-inelastic scattering process.[2] If so, cross sections of the following type:

$$e^-+e^+ \to p+\text{"anything,"}$$

where, for example, p is a proton, may be very large compared to those for two-body final states just as they are for the deep-inelastic scattering in comparison with elastic electron-proton scattering. This will mean sizable counting rates and many optimistic prospects for electron-positron colliding rings at high energies now under construction or in planning.[3]

In the first paper[1] of the present series of papers the general program of our work based on canonical field theory for studying inelastic lepton processes was described with primary emphasis placed on ideas, assumptions, and implications. Detailed calculations were omitted in order to present a clear and unified picture for various lepton-hadron scattering and lepton pair-annihilation processes in the very deep inelastic region. In the second paper we described the detailed derivation and formulation of the "parton model" for the deep-inelastic electron-nucleon scattering. In this third paper of the series we concentrate our effort on the corresponding "parton model" derivation and formulation for deep-inelastic electron-positron annihilation into a nucleon plus anything else and its precise relation to deep-inelastic electron-nucleon scattering. We derive the parton model and differentiate general predictions of scaling properties from specific numerical results in Sec. III. Other implications for electron-positron colliding-beam experiments, including a suggestion of an ideal and simple method of testing the unitary-symmetry scheme of strong interactions, are also presented and discussed in Sec. IV. In Appendix A we discuss the reasons that prevented us from formulating the annihilation problem in terms of commutators as did Bjorken for the scattering and why, therefore, we were driven to develop a canonical-field-theory model in order to accomplish the crossing.

II. ELECTRON-POSITRON ANNIHILATION AND GENERAL CROSSING

The physical process to be studied in this paper is the annihilation of electron-positron pairs to a nucleon with fixed momentum (but any polarization) plus "anything"—i.e., the process

$$e^-+e^+ \to p+\text{"anything."} \quad (1)$$

The detected nucleon, for definiteness, will be referred to as a proton. The notation "anything" indicates all possible hadrons including other protons. We shall work to lowest order in the fine-structure constant. The hadron structure probed in this process is summarized

* Work supported by the U. S. Atomic Energy Commission.

[1] S. D. Drell, D. J. Levy, and T. M. Yan, Phys. Rev. Letters 22, 744 (1969); Phys. Rev. 187, 2159 (1969); Phys. Rev. D 1, 1035 (1970). The last two papers will be referred to as Paper I and Paper II, respectively.

[2] J. D. Bjorken, Phys. Rev. 179, 1547 (1969).

[3] We thank B. Richter for a discussion of colliding electron-positron rings in operation or under construction.

in two structure functions defined by

$$\bar{W}_{\mu\nu}=4\pi^2\frac{E_p}{M}\sum_n\langle 0|J_\mu(0)|Pn\rangle\langle Pn|J_\nu(0)|0\rangle \times(2\pi)^4\delta^4(q-P-P_n)$$
$$=-\left(g_{\mu\nu}-\frac{q_\mu q_\nu}{q^2}\right)\bar{W}_1(q^2,\nu)+\frac{1}{M^2}\left(P_\mu-\frac{P\cdot q}{q^2}q_\mu\right)\times\left(P_\nu-\frac{P\cdot q}{q^2}q_\nu\right)\bar{W}_2(q^2,\nu), \quad (2)$$

where $|Pn\rangle$ is a state of one proton plus other hadrons with quantum numbers summarized by n. In (2) a spin average over the detected proton is understood; P_μ and q_μ are the four-momenta of the detected proton and the virtual photon, respectively; $q^2>0$ is the square of the photon's mass and $M\nu\equiv P\cdot q$ is the total energy transfer to hadrons in the rest system of the detected proton; and $J_\mu(x)$ is the total hadronic electromagnetic current. Unless we want to entertain the possibility of C, or T, violation in the hadronic electromagnetic interactions, we can equally well talk about an emerging proton, or antiproton, in the final state[4] of (1).

The structure functions $\bar{W}_{1,2}(q^2,\nu)$ are analogous to the structure functions $W_{1,2}(q^2,\nu)$ defined for electron-proton scattering:

$$W_{\mu\nu}=4\pi^2\frac{E_p}{M}\sum_n\langle P|J_\mu(0)|n\rangle\langle n|J_\nu(0)|P\rangle \times(2\pi)^4\delta^4(q+P-P_n)$$
$$=-\left(g_{\mu\nu}-\frac{q_\mu q_\nu}{q^2}\right)W_1(q^2,\nu)+\frac{1}{M^2}\left(P_\mu-\frac{P\cdot q}{q^2}q_\mu\right)\times\left(P_\nu-\frac{P\cdot q}{q^2}q_\nu\right)W_2(q^2,\nu), \quad (3)$$

where $|P\rangle$ is a one-nucleon state with four-momentum P_μ, q_μ is the four-momentum of the virtual photon, $q^2\equiv -Q^2<0$ is the square of the virtual photon's mass, and $M\nu\equiv P\cdot q$ is the energy transfer to the proton in the laboratory system. An average over the nucleon spin is also understood in the definition $W_{\mu\nu}$.

The kinematical region for (1) in the q^2, $M\nu$ plane is bounded as follows. For a fixed collision energy $q^2>4M^2$; the value of ν is bounded below by $\nu_{\min}=\sqrt{q^2}$, corresponding to the detected proton at rest in the c.m. system of the colliding-ring system, and is bounded above by $2M\nu_{\max}=q^2$, corresponding to the "elastic" process $e^-+e^+\to p+\bar{p}$. Thus $0<2M\nu/q^2<1$ for process (1). We recall that for inelastic electron-proton scattering, $1<2M\nu/Q^2<\infty$. For convenience the same symbol

[4] This means that such a difference should be probed for experimentally. If one is found, we would have to rule out the possibility that it is due to higher-order electromagnetic contributions before interpreting it as C violation. For general tests, see also A. Pais and S. Treiman, Phys. Letters **29B**, 308 (1969); Phys. Rev. **187**, 2076 (1969).

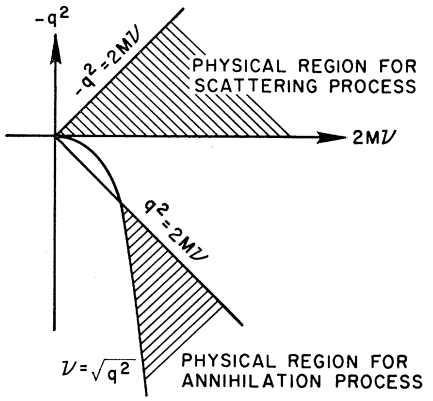

FIG. 1. Physical regions in the $(-q^2, 2M\nu)$ plane corresponding to inelastic scattering from a proton and to e^-e^+ annihilation to a proton.

w is used to denote $2M\nu/q^2$ for annihilation and $2M\nu/Q^2$ for scattering. The limit $w=1$ corresponds to the elastic processes $e+p\to e'+p'$ in scattering and $e^-+e^+\to p+\bar{p}$ in annihilation. Since we are interested in the deep inelastic continuum and not the resonance excitations, we require $2M\nu-Q^2\gg M^2$ for scattering and $q^2-2M\nu\gg M^2$ for annihihilation, i.e., we shall always assume $|q^2(w-1)|\gg M^2$. The point $w=1$ will only be approached from both sides. The regions of the $(q^2,2M\nu)$ plane corresponding to physical scattering and annihilation processes are shown in Fig. 1. In the colliding-ring or c.m. frame, the differential cross section for (1) is given by

$$\frac{d^2\sigma}{dE\,d\cos\theta}=\frac{4\pi\alpha^2}{(q^2)^2}\frac{M^2\nu}{\sqrt{q^2}}\left(1-\frac{q^2}{\nu^2}\right)^{1/2}\times\left[2\bar{W}_1(q^2,\nu)+\frac{2M\nu}{q^2}\left(1-\frac{q^2}{\nu^2}\right)\frac{\nu\bar{W}_2(q^2,\nu)}{2M}\sin^2\theta\right], \quad (4)$$

where E is the energy of the detected proton and θ is the angle of the proton momentum $\mathbf{P}$ with respect to the axis defined by the incident colliding e^- and e^+ beams.

On general grounds, Bjorken[2] has argued that in the deep inelastic region of large Q^2 and $M\nu$, the structure functions W_1 and νW_2 for electron scattering should become universal functions of one single variable w. The parton model derived in Papers I and II for deep-inelastic electron scattering gives a natural explanation to such a universal behavior on the basis of canonical field theory. A basic ingredient in the derivation of the parton model was the assumption that there exists an asymptotic region in which Q^2 can be made greater than the transverse momenta of all the particles involved, i.e., of the pions and nucleons that are the (virtual) constituents or "partons" of the proton.

One of the primary goals of the present paper is the study of the relation between $\bar{W}_{1,2}$ and $W_{1,2}$. We shall show in the following that under the same assumptions required in the study of inelastic scattering the structure

functions $\bar{W}_1$ and $\nu\bar{W}_2$ also have a Bjorken limit; i.e., they too become universal functions of the ratio $2M\nu/q^2$ for large q^2 and $M\nu$ in the annihilation region of Fig. 1. In this limit we can derive a parton model for the $\bar{W}$ from canonical field theory. Furthermore, we shall also show that the structure functions W_1 and νW_2 for inelastic scattering as measured or calculated near $w\sim 1$ give predictions to the annihilation process (1) near $2M\nu/q^2\sim 1$. Since the data on electron-proton scattering from SLAC and DESY[5] seem to support at least qualitatively Bjorken's original suggestion, we reach the important conclusion that the structure functions $\bar{W}_1$ and $\nu\bar{W}_2$ should also be expected to exhibit similar universal behavior at high energies with the structure functions for annihilation closely related to those for scattering. The precise connection will be given later.

By straightforward application of the reduction formalism to the proton P in the states in (2) and (3) it is readily shown that $W_{\mu\nu}$ and $\bar{W}_{\mu\nu}$ are related by the substitution law

$$\begin{aligned}\bar{W}_{\mu\nu}(q,P)&=-W_{\mu\nu}(q,-P)\,,\\ \bar{W}_1(q^2,\nu)&=-W_1(q^2,-\nu)\,,\\ \nu\bar{W}_2(q^2,\nu)&=(-\nu)W_2(q^2,-\nu)\,.\end{aligned}\tag{5}$$

Let us write for spacelike q^2

$$MW_1(q^2,\nu)=F_1(w,s)\,,\quad \nu W_2(q^2,\nu)=F_2(w,s)\,,\tag{6}$$

where $w\equiv 2M\nu/-q^2>1$ and $s\equiv(q+P)^2=2M\nu-Q^2+M^2>M^2$. In the Bjorken limit ($\lim_{\mathrm{Bj}}$), we have

$$\begin{aligned}\lim_{\mathrm{Bj}} MW_1(q^2,\nu)&=F_1(w)=\lim_{s\to\infty}F_1(w,s)\,,\\ \lim_{\mathrm{Bj}} \nu W_2(q^2,\nu)&=F_2(w)=\lim_{s\to\infty}F_2(w,s)\quad(w>1)\,.\end{aligned}\tag{7}$$

The substitution law (5) gives for timelike q^2

$$M\bar{W}_1(q^2,\nu)=-F_1(w,s)\,,\quad \nu\bar{W}_2(q^2,\nu)=F_2(w,s)\,,\tag{8}$$

where $0<w=2M\nu/q^2<1$ and $s=(q-P)^2=q^2-2M\nu+M^2>M^2$. If we can show that the Bjorken limit exists for timelike q^2, we may also expect to find

$$\begin{aligned}\lim_{\mathrm{Bj}}(-)M\bar{W}_1(q^2,\nu)&=\bar{F}_1(w)=\lim_{s\to\infty}F_1(w,s)=F_1(w)\,,\\ \lim_{\mathrm{Bj}}\nu\bar{W}_2(q^2,\nu)&=\bar{F}_2(w)=\lim_{s\to\infty}F_2(w,s)=F_2(w)\,,\end{aligned}\tag{9}$$

namely, $\bar{F}_1(w)$ and $\bar{F}_2(w)$ are the continuations of the corresponding functions $F_1(w)$ and $F_2(w)$ from $w>1$ to $w<1$. Relations (9) will be true, for example, if the Bjorken limits are approached algebraically so the sign change in $w-1$ between $w>1$ for scattering and $0<w<1$ for pair annihilation will not have any pathological effect. We shall now demonstrate, using as an example the model developed in Ref. 1 of charge-symmetric theory of pseudoscalar pions and nucleons with γ_5 coupling and with a transverse momentum cutoff, that, first, the Bjorken limits of $\bar{W}_1$ and $\nu\bar{W}_2$ exist, and, second, the relations (9) are indeed satisfied. The failure of more general attempts to accomplish this crossing is described in Appendix A. The demonstration of Bjorken limiting behavior will closely parallel the derivation given in Paper II for deep-inelastic scattering. Explicit verification of (9) as the continuation of the scale functions from $w>1$ to $w<1$ will be displayed in Appendix B through fourth order in the strong interactions. For the particular set of ladder graphs it will be shown to all orders.

III. DERIVATION OF PARTON MODEL FOR DEEP-INELASTIC ELECTRON-POSITRON ANNIHILATION

To make apparent the connection between the deep-inelastic electron-positron annihilation process (1) and the deep-inelastic electron-proton scattering, we will study the annihilation process (1) in an infinite-momentum frame of the detected proton, just as the electron scattering was in an infinite-momentum frame of the initial proton. A convenient infinite-momentum frame for this analysis is one in which the current introduces a large momentum of the order of magnitude of $\sqrt{q^2}$ transverse to the direction of the momentum $\mathbf{P}\to\infty$ of the detected proton. This is analogous to the situation exploited in our study of the deep-inelastic scattering which also was analyzed in a coordinate frame in which the current introduced a large transverse momentum, $\sqrt{Q^2}$, relative to the infinite momentum of the initial proton. For the scattering as viewed in a reference frame with this property there emerged two distinct groups of final hadronic particles: one group with a limited transverse momentum relative to $\mathbf{P}$ because of our cutoff $k_{\max}\ll|q|$, and a second group with its components of momenta transverse to $\mathbf{P}$ clustered about the asymptotically large value $\propto|q|$ (see Fig. 8 of Paper II). A similar grouping of final hadrons will occur in the annihilation process.

We shall take the infinite-momentum limit in the same manner as in Paper II for the scattering analysis by first letting $P\to\infty$ and *then* taking the limit q^2, $M\nu\to\infty$, so that $q^2/P, M\nu/P\to 0$. The defining relations

$$q_\mu q^\mu=q^2>0\,,\quad q\cdot P=M\nu\tag{10}$$

are then satisfied up to corrections of order $w^{-1}(M/\nu)$ if we specify the momentum components to be

$$\begin{aligned}P^\mu&=(P+M^2/2P,0,0,P)\,,\\ q^\mu&=\left(P\frac{f+1}{w}+\frac{2M\nu-q^2}{4P},\mathbf{q}_\perp,P\frac{f+1}{w}-\frac{2M\nu+q^2}{4P}\right),\\ q_\perp{}^2&=fq^2\,,\end{aligned}\tag{11}$$

[5] E. Bloom *et al.*, Phys. Rev. Letters **23**, 930 (1969); M. Breidenbach *et al.*, *ibid.* **23**, 935 (1969); W. Albrecht *et al.*, DESY Report No. 69/7 (unpublished). See in particular the report by R. Taylor, Daresbury Conference on Electrons and Photons, SLAC Report No. SLAC PUB-677, 1969 (unpublished).

where $f\geq 0$ measures transverse momentum (squared) introduced by the current. Any value of $f>0$ will satisfy our above criterion for producing two distinct groups of final hadrons. For simplicity we shall specify $f=1$. Any other choice will do. In fact, it *must* do if the calculations and the cutoff procedure as formulated in Paper II are to be acceptable.[6] That this is indeed the case we have verified by explicit construction. Indeed, the results of this paper as originally reported in Paper I were first derived in the coordinate frame obtained from (11) by setting $f=0$.[7]

By analogy with our discussion of electron scattering, we undress the electromagnetic current operator $J_\mu(x)$ by the familiar U transformation

$$J_\mu(x)=U^{-1}(t)j_\mu(x)U(t)\,, \tag{12}$$

with

$$U(t)=\left(\exp\left[-i\int_{-\infty}^{t}dt\,H_I(t)\right]\right)_+\,. \tag{13}$$

In our model the interaction Hamiltonian H_I and the electromagnetic current J_μ are, respectively,

$$H_I(t)=ig\int d^3x\,\bar{\psi}(x)\gamma_5\boldsymbol{\tau}\psi(x)\cdot\boldsymbol{\pi}(x)\,, \tag{14}$$

$$J_\mu(x)=\bar{\psi}_p\gamma_\mu\psi_p+i\pi^+\overleftrightarrow{\partial}_\mu\pi^-\,. \tag{15}$$

As in the study of inelastic electron scattering, the definition of the interaction Hamiltonian (14) involves implicitly the fundamental assumption that there exists a transverse momentum cutoff at each strong vertex.

Before proceeding further, we recall from Paper II certain basic properties simplifying the application of old-fashioned perturbation theory in an infinite-momentum frame, and, in particular, with the interaction (14). In the old-fashioned perturbation theory a physical process is described by a sum of infinite series of terms ("diagrams") with a time-ordered sequence of events represented by the vertices. Every intermediate state between two consecutive vertices is associated with an energy denominator. In the perturbation-series expansion all disconnected diagrams may be consistently omitted, as explained in Paper II. Moreover, an energy denominator in an infinite-momentum frame is of order $1/P$ if all the particles in the particular intermediate state move forward in the direction of the initial infinite momentum; the energy denominator becomes of order P if any of the intermediate particles have a negative longitudinal momentum. Thus, if all the vertices were finite in an infinite-momentum frame, this property of energy denominators would prevent any intermediate particle (real or virtual) from having negative longitudinal momentum. However, the interaction Hamiltonian (14) leads to vertices of order P when the two nucleons at a strong vertex have infinite longitudinal momenta opposite in sign [see Eq. (9) of Paper II]. As a result, a large energy denominator of order P corresponding to an intermediate state with particle(s) moving backward can be compensated by two large strong vertices.

On the other hand, for the "good components" of j_μ—i.e., the time and third component along the reference infinite-momentum four-vector—no extra power of P will be introduced into the numerator if the two particles at an electromagnetic vertex have longitudinal momenta opposite in sign. Consequently, in the following analysis only good components of j_μ will be considered. This is sufficient for us to obtain the two structure functions $\bar{W}_{1,2}$ by computing $\bar{W}_{00}$ and $\bar{W}_{33}$. The whole tensor $\bar{W}_{\mu\nu}$ may then be reconstructed by relativistic covariance. We now substitute (12) into (2) and obtain

$$\bar{W}_{\mu\nu}=4\pi^2\frac{E_p}{M}\sum_n\langle 0|U^{-1}j_\mu(0)U|Pn\rangle\langle nP|U^{-1}j_\nu(0)U|0\rangle \times(2\pi)^4\delta^4(q-P-P_n)\,, \tag{16}$$

where we define $U\equiv U(0)$. For the good components of j_μ ($\mu=0$ or 3) along $\mathbf{P}$, the effect of U on the vacuum state may be ignored. If $U(0)$ operates on the vacuum state, it must produce a baryon pair plus meson with zero total momentum so that at least one particle will move toward the left and another toward the right along $\mathbf{q}$ or $\mathbf{P}$ in (16). Thus the energy denominators will be of order $\sim P$ instead of $\sim 1/P$. However, when working with the good components of the current—i.e., j_0 or j_3 along $\mathbf{P}$—no compensating factors of P are introduced into the numerator by the vertices and so such terms can be neglected in the infinite-momentum limit. To illustrate this result, we consider the example drawn in the diagram of Fig. 2(a), where a nucleon-antinucleon pair plus one meson are created from the vacuum and the nucleon current is operating. At least one large energy denominator of order P is introduced by this intermediate state. It then requires at least two compensating powers of P in the numerator to overcome. One factor of P can be supplied by the strong vertex from which these particles are created if the

---

[6] There is a similar arbitrariness in choosing the coordinate system for analyzing the deep-inelastic scattering. A simple calculation verifies that for all $f\geq 0$, with $Q^2\equiv -q^2>0$, the components of q^μ and P^μ can be specified by

$$P^\mu=(P+M^2/2P,\,0,\,0,\,P),$$
$$q^\mu=\left(P\frac{f-1}{w}+\frac{2M\nu-Q^2}{4P},\,\mathbf{q}_1,\,P\frac{f-1}{w}-\frac{2M\nu+Q^2}{4P}\right),$$
$$q_1^2=fQ^2.$$

The analysis of Paper II for inelastic scattering was carried through for $f=1$ although we could just as well have fixed $f=0$. With the latter choice, the separation of the final hadrons into two groups would have been on the basis of a longitudinal- rather than a transverse-momentum mismatch.

[7] More precisely, we wrote in Paper I

$$q^\mu=(P/w+M\nu/P,\,0,\,0,\,P/w),$$

which also satisfied (10). In this frame, the separation of final hadrons into two groups is by their longitudinal-momentum difference and identical results are obtained.

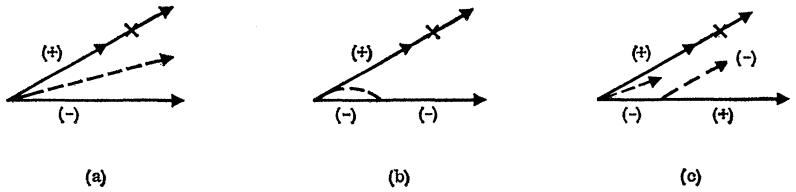

FIG. 2. Examples of diagrams which cannot contribute to $\bar{W}_{\mu\nu}$ when only good currents are used. (+) and (−) indicate the sense of longitudinal momentum.

nucleon and the antinucleon have longitudinal momenta opposite in sign. Nevertheless, it is impossible to obtain another compensating factor of P when only the good components of j_μ are employed [Eq. (16)]. The only possibility left is to produce another large strong vertex by changing the sign of the longitudinal momentum of one of the nucleon pair before the current operates (if after the current operates, then *two* large energy denominators instead of one are introduced). This is impossible either because spatial momentum is conserved at each vertex [Fig. 2(b)], or it will introduce additional large energy denominators [Fig. 2(c)]. The same conclusion holds for pion-current contributions. As discussed in Paper II, more interaction vertices to higher order in the strong interactions cannot compensate for the lost powers of P. We conclude, therefore, in the infinite-momentum frame (11), that Eq. (16) becomes, for good currents,

$$\bar{W}_{\mu\nu}=4\pi^2\frac{E_p}{M}\sum_n\langle 0|j_\mu(0)U|Pn\rangle\langle nP|U^{-1}j_\nu(0)|0\rangle \times(2\pi)^4\delta^4(q-P-P_n). \quad (17)$$

Other simplifications which follow from working in an infinite-momentum frame are similar to those discussed in Paper II. For example, if a particle is created at a strong vertex moving opposite to the initial infinite longitudinal momentum, it must change its direction of motion or be annihilated at the next vertex; such a particle can never traverse beyond a strong vertex without being disturbed. As the equations for the electromagnetic vertices show [see Eq. (10) of Paper II], to leading order the good components of the current will create a pair with both particles moving with positive longitudinal-momentum components along the direction of q_3 and P. Moreover, all *final* particles produced in state $|Pn\rangle$ in (17) from the current must have positive longitudinal momenta along $\mathbf{P}$ as a result of energy-momentum conservation enforced by the δ function in (17). In addition, the longitudinal momenta of the intermediate particles are generally restricted to certain finite ranges or fractions of the incident momenta. For the detailed discussion the reader is referred to Paper II.

The derivation of a parton model for (1) can be carried out in very close parallel to the one given in Paper II for inelastic electron scattering. There are only minor differences between the two cases, arising from the fact that the virtual photon is spacelike in the scattering and timelike in the annihilation process.

To maximize the similarity with the scattering development in Paper II, we choose $f=1$ in (11), so that

$$q^\mu=\left(\frac{2P}{w}+\frac{2M\nu-q^2}{4P},\ \mathbf{q}_\perp,\ \frac{2P}{w}-\frac{2M\nu+q^2}{4P}\right), \quad q_\perp{}^2=q^2, \quad (18)$$

and take the analogous Bjorken limit

$$q^2, M\nu\to\infty:\quad 0<2M\nu/q^2\equiv w<1.$$

Again the final particles of the annihilation process (1) in the infinite-momentum frame (18) are divided into two well-separated groups of particles. One group of particles contains the detected proton and moves closely along the direction of its momentum $\mathbf{P}$; the other group of particles also moves close to each other but along a direction differing from the direction of P by a large transverse momentum of order $\sqrt{q^2}$. In the Bjorken limit, as in the scattering case, there is no interaction or interference between these two groups of particles. Consequently, only two general classes of diagrams as shown in Fig. 3 remain in (17).

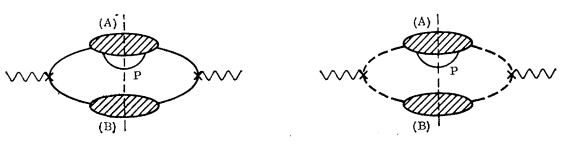

FIG. 3. The two general classes of diagrams which contribute to $\bar{W}_{\mu\nu}$ in the Bjorken limit.

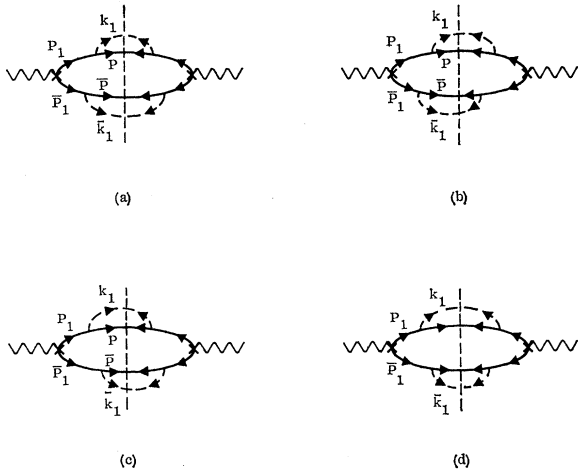

FIG. 4. Typical examples of diagrams which contribute to $\bar{W}_{\mu\nu}$.

To gain an understanding of how the expression (17) and the kinematics simplify in the Bjorken limit, we calculate explicitly a few terms in (17) represented by diagrams of Fig. 4 in which all the pions are assumed to be neutral. The diagrams in Figs. 4(a)–4(d) are associated with a common final state and have identical topological structure but have different time ordering among the strong vertices. The contributions to $\bar{W}_{\mu\nu}$ are, respectively,

$$\bar{W}_{\mu\nu}{}^{(a;b;d)}=\left(\frac{g^2}{(2\pi)^3}\right)^2\frac{1}{4M}\int\frac{d^3k_1}{2\omega_1}\frac{d^3\bar{k}_1}{2\bar{\omega}_1}\delta(q^0-E_p-\bar{E}-\omega_1-\bar{\omega}_1)\frac{1}{(2E_1)^2(2\bar{E}_1)^2(2\bar{E})}$$
$$\times\frac{T_{\mu\nu}}{(E_p+\bar{E}+\omega_1+\bar{\omega}_1-E_1-\bar{E}_1)^2}\left(\frac{1}{(E_p+\omega_1-E_1)^2};\frac{1}{(E_p+\omega_1-E_1)(\bar{E}+\bar{\omega}_1-\bar{E}_1)};\frac{1}{(\bar{E}+\bar{\omega}_1-\bar{E}_1)^2}\right), \quad (19)$$

$$\bar{W}_{\mu\nu}{}^{(b)}=\bar{W}_{\mu\nu}{}^{(c)}, \quad (20)$$

where

$$T_{\mu\nu}=T_{\nu\mu}=(-)\,\mathrm{Tr}\{(M+\gamma P)\gamma_5(M+\gamma P_1)\gamma_\mu(M-\gamma\bar{P}_1)\gamma_5(M-\gamma\bar{P})\gamma_5(M-\gamma\bar{P}_1)\gamma_\nu(M+\gamma P_1)\gamma_5\}. \quad (21)$$

Observe the identity

$$\frac{1}{(E_p+\omega_1-E_1)^2}+\frac{2}{(E_p+\omega_1-E_1)(\bar{E}_p+\bar{\omega}_1-\bar{E}_1)}+\frac{1}{(\bar{E}+\bar{\omega}_1-\bar{E}_1)^2}=\frac{(E_p+\bar{E}+\omega_1+\bar{\omega}_1-E_1-\bar{E}_1)^2}{(E_p+\omega_1-E_1)^2(\bar{E}+\bar{\omega}_1-\bar{E}_1)^2}. \quad (22)$$

Evaluating the trace and using (22), we obtain

$$\bar{W}_{\mu\nu}{}^{(2)}=\bar{W}_{\mu\nu}{}^{(a)}+\bar{W}_{\mu\nu}{}^{(b)}+\bar{W}_{\mu\nu}{}^{(c)}+\bar{W}_{\mu\nu}{}^{(d)}=\left(\frac{g^2}{(2\pi)^3}\right)^2\frac{1}{4M}\int\frac{d^3k_1}{2\omega_1}\frac{d^3k_1}{2\bar{\omega}_1}\delta(q^0-E_p-\bar{E}-\omega_1-\bar{\omega}_1)$$
$$\times\frac{(-2)^2(M^2-\bar{P}\cdot\bar{P}_1)(M^2-P\cdot P_1)2[-g_{\mu\nu}(M^2+P_1\cdot\bar{P}_1)+(P_{1\mu}\bar{P}_{1\nu}+P_{1\nu}\bar{P}_{1\mu})]}{(2E_1)^2(2\bar{E}_1)^2(2\bar{E})(E_p+\omega_1-E_1)^2(\bar{E}+\bar{\omega}_1-\bar{E}_1)^2}. \quad (23)$$

We adopt the following parametrization:

$$\mathbf{P}_1=\eta_1\mathbf{P}+\mathbf{k}_{1\perp},\quad \mathbf{k}_1=(\eta_1-1)\mathbf{P}+\mathbf{k}_{1\perp},$$
$$\bar{\mathbf{P}}=\eta\bar{\mathbf{P}}_1+\mathbf{k}_\perp,\quad \bar{\mathbf{k}}_1=(1-\eta)\bar{\mathbf{P}}_1-\mathbf{k}_\perp. \quad (24)$$

This parametrization is designed to make the analogy to the inelastic scattering as close as possible by following along the nucleon line with the detected proton as the starting point and scaling the adjacent nucleon's momentum with respect to that of the preceding one. [Compare (23) and (24) with Eqs. (58) and (52) of Paper II.] Notice that the differences $(E_p+\omega_1-E_1)$ and $(\bar{E}+\bar{\omega}_1-\bar{E}_1)$ can be ignored in the energy-conserving δ function of (23), since

$$E_p+\omega_1-E_1=\left(P+\frac{M^2}{2P}\right)+\left((\eta_1-1)P+\frac{k_{1\perp}{}^2+\mu^2}{2(\eta_1-1)P}\right)-\left(\eta_1P+\frac{k_{1\perp}{}^2+M^2}{2\eta_1P}\right)$$
$$=\frac{k_{1\perp}{}^2+M^2(\eta_1-1)^2+\mu^2\eta_1}{2\eta_1(\eta_1-1)P}, \quad (25)$$
$$\bar{E}+\bar{\omega}-\bar{E}_1=\frac{k_\perp{}^2+M^2(1-\eta)^2+\mu^2\eta}{2\eta(1-\eta)P}$$

are small as compared with the term $(2M\nu-q^2)/4P$ appearing in q^0. Thus energy is conserved to leading order across the electromagnetic vetex:

$$\delta(q^0-E_p-\bar{E}-\omega_1-\bar{\omega}_1)\approx\delta(q^0-E_1-\bar{E}_1)$$
$$=(2\bar{E}_1)\delta(2M\nu\eta_1-q^2)$$
$$=(2\bar{E}_1)\delta(2P_1\cdot q-q^2), \quad (26)$$

where the following approximation valid in the Bjorken limit has been used:

$$\bar{E}_1=[(\mathbf{q}-\mathbf{P}_1)^2+M^2]^{1/2}\approx[(q_3-\eta_1P)^2+q_1{}^2]^{1/2}$$
$$=q_3-\eta_1P+q_1{}^2/2(q_3-\eta_1P). \quad (27)$$

In (27), $q_3-\eta_1P>0$ since the pair must move along $\mathbf{P}$ as discussed below (17).

Combining (23), (24), and (26), and ignoring terms proportional to q_μ or q_ν, we obtain for the numerator factor in (23)

$$2[-g_{\mu\nu}(M^2+P_1\cdot\bar{P}_1)+(P_{1\mu}\bar{P}_{1\nu}+P_{1\nu}\bar{P}_{1\mu})]$$
$$=-g_{\mu\nu}q^2-4\eta_1{}^2P_\mu P_\nu$$
$$=-g_{\mu\nu}q^2-4(1/w)^2P_\mu P_\nu, \quad (28)$$

and from this we find

$$\nu\bar{W}_2^{(2)}=(1-Z_{2(\pi^0)})\Big[-\frac{g^2}{16\pi^2}\frac{1}{w}\Big(\frac{1}{w}-1\Big)\times\int dk_{1\perp}^2\frac{k_{1\perp}^2+M^2(1-1/w)^2}{[k_{1\perp}^2+M^2(1-1/w)^2+\mu^2/w]^2}\Big],\quad(29)$$

$$\bar{W}_1^{(2)}=-(w/2M)(\nu\bar{W}_2^{(2)}),$$

where

$$Z_{2(\pi^0)}=1-\frac{g^2}{16\pi^2}\int dk_\perp^2\int_0^1 d\eta(1-\eta)\times\frac{k_\perp^2+M^2(1-\eta)^2}{[k_\perp^2+M^2(1-\eta)^2+\mu^2\eta]^2}\quad(30)$$

is the wave-function renormalization constant for a proton due to a one-proton-plus-one-neutral-pion intermediate state. [See Eq. (18) of Paper II.] Equation (29) can be rewritten as

$$\bar{W}_{\mu\nu}^{(2)}+Z_{2(\pi^0)}\bar{W}_{\mu\nu}^{(1)}=\bar{W}_{\mu\nu}^{(1)},\quad(31)$$

where $\bar{W}_{\mu\nu}^{(1)}$ is the contribution of a diagram obtained from Fig. 4 by replacing the group of particles deflected from $\mathbf{P}$ by $\mathbf{q}_\perp$ with a single proton. This simple example provided by Fig. 4 actually contains all the essential characteristics of the Bjorken limit in the annihilation process. They are: (i) The pair produced by the current j_μ and all the particles in final states $|Pn\rangle$ must have positive longitudinal momenta along the direction of $\mathbf{q}$ or $\mathbf{P}$; (ii) in the Bjorken limit the over-all energy-conserving δ function in (17) can be replaced by conservation across the electromagnetic vertex as in (25); (iii) the two groups of particles (A) and (B) in Fig. 3 that are produced are well separated and well identified by a transverse-momentum difference $\propto q$; and (iv) the relative time ordering between events which occur in one group and events in the other may be ignored. The U matrix acts independently and separately on the two groups of particles. Summing over all possible combinations of particles in group (B), one obtains unity for the total probability for anything to happen. Equation (31) is an example of this kind. It states that the net effect of the U matrix on group (B) is unity after summation over all possibilities in this group. In this case, summation of the four different time orderings as shown in Fig. 4 with two-particle states in (B) precisely cancels the wave-function renormalization effect Z_2 of the single antiproton state in (B).

The four properties described above have their analogs in the inelastic scattering case and were discussed in more detail in Paper II. According to (ii), the state $U|Pn\rangle$ may be treated as an eigenstate of the total Hamiltonian with eigenvalue E_p+E_n and (17) becomes, with the aid of the translation operators,

$$\lim_{\mathrm{Bj}}\bar{W}_{\mu\nu}=4\pi^2\frac{E_p}{M}\int(dx)e^{iqx}\times\sum_n\langle 0|j_\mu(0)e^{-i(P+P_n)x}U|Pn\rangle\times\langle nP|U^{-1}j_\nu(0)|0\rangle$$
$$=4\pi^2\frac{E_p}{M}\int(dx)e^{+iqx}\sum_n\langle 0|j_\mu(x)U|Pn\rangle\times\langle nP|U^{-1}j_\nu(0)|0\rangle.\quad(32)$$

According to (iv), the final result of (32) is equivalent to retaining only those terms in which the group with deflected momenta contains only one charged particle ($\pi^\pm$, p, or $\bar{p}$ in our model), which we shall denote by λ. Therefore,

$$\lim_{\mathrm{Bj}}\bar{W}_{\mu\nu}=4\pi^2\frac{E_p}{M}\int(dx)e^{+iqx}\times\sum_n\sum_{\lambda=\pi^\pm,p,\bar{p}}\langle 0|j_\mu(x)|\lambda,U(Pn)\rangle\times\langle(nP)U^{-1},\lambda|j_\nu(0)|0\rangle.\quad(33)$$

This is the parton result for the annihilation process (1). The similarity of (33) with the corresponding expression for inelastic scattering in the Bjorken limit is clear by a comparison of graphs in Fig. 5: (a) with (c) and (b) with (d).

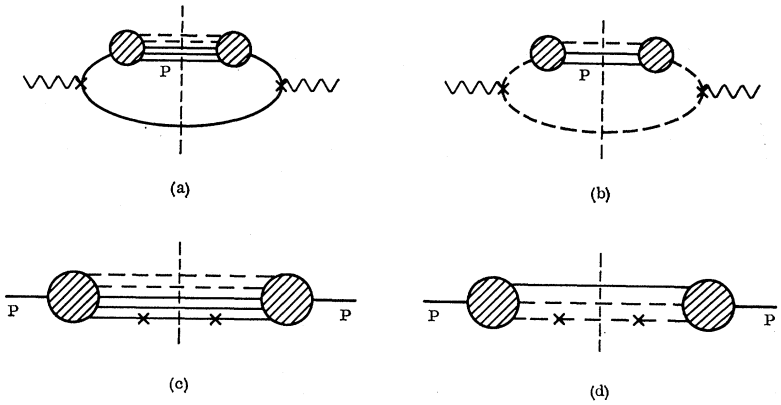

FIG. 5. Comparison between the general classes contributing to the scattering and those to the annihilation.

Every term in (33) is represented by a diagram of the form shown by Figs. 5(a) and 5(b) for a nucleon-current and pion-current contribution, respectively. The evaluation of (33) then obviously involves the matrix elements

$$\int (dx)e^{iqx}\sum_{\bar{P}_n,\bar{s}}\langle 0|j_\mu(x)|\bar{P}_n\bar{s};P_ns\rangle\langle s'P_n;\bar{s}\bar{P}_n|j_\nu(0)|0\rangle$$
$$=\frac{-1}{4\pi^2}\frac{2M}{2E_n}\delta(q^2-2P_n\cdot q)\bar{u}_{P_n}(s')\gamma_\nu \times[M-\gamma(q-P_n)]\gamma_\mu u_{P_n}(s) \quad (34)$$

for a nucleon-current contribution, and

$$\int (dx)e^{iqx}\sum_{k_n}\langle 0|j_\mu(x)|k_n,\bar{k}_n\rangle\langle\bar{k}_n,k_n|j_\nu(0)|0\rangle$$
$$=\frac{1}{4\pi^2}\frac{1}{2\omega_n}\delta(q^2-2k_n\cdot q)(2k_{n\mu}-q_\mu)(2k_{n\nu}-q_\nu) \quad (35)$$

for a pion-current contribution. In these two equations, P_n, $\bar{P}_n$ and k_n, $\bar{k}_n$ are the momenta of the proton-antiproton pair and pion pair, respectively; s, $\bar{s}$ are the spins of the proton and antiproton, respectively. Equation (34) may be simplified to obtain

$$\int (dx)e^{iqx}\sum_{\bar{P}_n,\bar{s}}\langle 0|j_\mu(x)|\bar{P}_n\bar{s};P_ns\rangle\langle s'P_n;\bar{s}\bar{P}_n|j_\nu(0)|0\rangle$$
$$=\frac{1}{4\pi^2}\frac{1}{2E_n}\delta(q^2-2P_n\cdot q) \times[(-2P_n\cdot q)g_{\mu\nu}-4P_{n\mu}P_{n\nu}]\delta_{ss'}. \quad (36)$$

Ignoring terms proportional to q_μ or q_ν, substituting $P_{n\mu}=\eta_nP_\mu$ in (36) and $k_{n\mu}=\eta_nP_\mu$ in (35), we obtain

$$\int (dx)e^{iqx}\sum_{\bar{P}_n,\bar{s}}\langle 0|j_\mu(x)|\bar{P}_n\bar{s};P_ns\rangle\langle s'P_n;\bar{s}\bar{P}_n|j_\nu(0)|0\rangle$$
$$=\frac{1}{4\pi^2}\frac{1}{2E_n}\delta(q^2-2M\nu\eta_n) \times\left[q^2(-g_{\mu\nu})-4\frac{1}{w^2}P_\mu P_\nu\right]\delta_{ss'}, \quad (37)$$

$$\int (dx)e^{+iqx}\sum_{k_n}\langle 0|j_\mu(x)|\bar{k}_n,k_n\rangle\langle k_n,\bar{k}_n|j_\nu(0)|0\rangle$$
$$=\frac{1}{4\pi^2}\frac{1}{2\omega_n}\delta(q^2-2M\nu\eta_n)4\frac{1}{w^2}P_\mu P_\nu. \quad (38)$$

In (37) and (38), η_n represents the "fraction" of the longitudinal momentum with respect to P of the charged particle created by the virtual photon which will eventually produce the detected proton.

The complete dependence of $\bar{W}_{\mu\nu}$ on q^2 and $M\nu$ has now been explicitly exhibited in (37) and (38). These two equations show that both $\bar{W}_1$ and $\nu\bar{W}_2$ are universal functions of one single variable w in the Bjorken limit:

$$\lim_{\mathrm{Bj}}M\bar{W}_1(q^2,\nu)=-\bar{F}_1(\omega),$$
$$\lim_{\mathrm{Bj}}\nu\bar{W}_2(q^2,\nu)=\bar{F}_2(w). \quad (39)$$

According to (37) and (38) the nucleon-current (or more generally any spin-$\frac{1}{2}$ current) contributions to $\bar{F}_{1,2}(w)$ have a fixed ratio

$$\bar{F}_1(w)/\bar{F}_2(w)=\tfrac{1}{2}w \quad (\text{spin-}\tfrac{1}{2}\text{ current}) \quad (40)$$

and the pion current (or more generally any spin-0 current) does not contribute to $\bar{F}_1(w)$:

$$\bar{F}_1(w)=0 \quad (\text{spin-0 current}). \quad (41)$$

Both relations (40) and (41) are independent of dynamical details. The relative importance of the nucleon- and pion-current contributions, and hence of $\bar{F}_1(w)$ and $\bar{F}_2(w)$, is determined by the dynamics, however.

Although it is not apparent that $\bar{F}_1(w)$ and $\bar{F}_2(w)$ computed from (33) are the same as $F_1(w)$ and $F_2(w)$ computed from (57) of Paper II and continued to $0<w<1$, it is actually so by explicit calculation. Verification is straightforward for second-order pion-current contributions as well as for the similar nucleon-current contributions which are displayed in (29) for comparison with $F_2^{(17a)}$ in the Appendix of Paper II.

We have also verified this explicitly to fourth order in g for diagrams with both pion- and nucleon-current contributions, and to any order for ladder diagrams with nucleon-current operating (Fig. 15 of Paper II) and its corresponding diagram [Fig. 8(u) in Appendix B] for annihilation process (1). In this verification we only have to identify the transverse-momentum cutoffs in both cases. The details of this verification and the cutoff prescription are presented in Appendix B.

We summarize the main conclusions of this section. First, to arrive at (33) we have exploited the nice properties of the good components of the electromagnetic current to make the discussion simple. But with the covariant tensor structures explicitly displayed as given in (37) and (38), the results are clearly applicable to all components. Equations (37) and (38) also show explicitly the scaling behavior of $\bar{W}_1$ and $\nu\bar{W}_2$ in the Bjorken limit. Second, although the analysis given here uses a specific field-theoretic model, (14) and (15), it is clear from the discussion of this section that the derivation of the parton-model result (33), the scaling behavior (39), and the characteristic feature of any spin-$\frac{1}{2}$ and spin-0 currents, (40) and (41), can be carried out for more general field-theoretic models as long as there exists a transverse-momentum cutoff at every strong vertex. This transverse-momentum cutoff is crucial in allowing us simply to do power counting in $1/q^2$ in order to identify leading terms, but the origin and form of this cutoff is irrelevant to these general

results. Third, we believe that the crossing relations (9) also have a more general validity although we are unable to construct a general proof. We say this because the substitution law (5) is a general property of any field theory, and since the Bjorken limits of both $W_{\mu\nu}$ and $\overline{W}_{\mu\nu}$ exist by our analysis, it is hard to imagine that they do not approach the same limiting functions. Our explicit verification to higher orders for a particular model in Appendix B lends support to this belief, but is of course no substitute for a proof.

IV. PREDICTIONS

We are now in a position to study the experimental implications of the results obtained in Sec. III. They may be summarized as follows:

(a) In the Bjorken limit, the differential cross section for the annihilation process (1) in the c.m. frame of the electron-positron pair becomes, using $E=M\nu/q^0=M\nu/\sqrt{q^2}$ and the definition $w=2M\nu/q^2$,

$$\frac{d^2\sigma}{dw\,d\cos\theta}=\tfrac{3}{2}\sigma_l[-F_1(w)+\tfrac{1}{4}wF_2(w)\sin^2\theta]w, \quad (42)$$

where

$$\sigma_l=\tfrac{1}{3}(4\pi\alpha^2/q^2)$$

is the total cross section of electron-positron annihilation into muon pairs, in the relativistic limit. Generally, knowledge about $F_{1,2}(w)$ for $w>1$ as determined by inelastic e-p scattering measurements does not provide any useful information for $0<w<1$ unless one knows the analytic forms of $F_{1,2}(w)$ exactly. However, $w=1$ is a common boundary for both scattering and annihilation. Therefore, with a mild assumption of smoothness, the ep deep-inelastic scattering data near $w\gtrsim 1$ predict completely the "deep"-inelastic annihilation process near $w\lesssim 1$. This connection is a far-reaching consequence of the Bjorken limit. The two processes occur in different and disjoint kinematical regions and are not related in general. Recall that $w=1$ corresponds to the two-body elastic channel and by w near 1 we mean $|q^2(w-1)|\gg M^2$.

(b) In the infinite-momentum frame (18), the secondary particles in the annihilation process (1) are divided into two well-defined groups, one with momenta along the direction of the detected nucleon and the other with a large transverse component of order q. The distribution of secondaries in the colliding-ring frame will look like two jets along and opposite to the direction of the momentum of the detected nucleon with typical transverse momenta $k_\perp\ll\sqrt{q^2}$ on the individual particles.

(c) Combining Eqs. (40) and (41) for $0<w<1$ and the analogous equations for $w>1$ [Eqs. (114) and (115) of Paper II] with relations (9), we conclude for any value of w $(0<w<\infty)$ that if the current interacts with a nucleon (or more generally any spin-$\frac{1}{2}$ particles), then

$$F_1(w)=\tfrac{1}{2}wF_2(w) \quad \text{(nucleon current)}, \quad (43)$$

and if the current interacts with a pion (or more generally any spin-0 particles), then

$$F_1(w)=0 \quad \text{(pion current)}. \quad (44)$$

Now, in (42) we may choose $\sin^2\theta=0$; thus it is necessary that

$$F_1(w)\leq 0, \quad 0<w<1. \quad (45)$$

On the other hand, $F_{1,2}(w)$ are non-negative for $w>1$. We conclude that both $F_1(w)$ and $F_2(w)$ change sign at $w=1$ if the nucleon current dominates, while $F_2(w)$ does not change sign at $w=1$ if the pion current dominates. We therefore predict near $w\sim 1$ that

$$F_2(w)=C_N(w-1)^{2n+1}, \quad n=0,1,\ldots \quad \text{(nucleon current)}, \quad (46)$$

$$F_2(w)=C_\pi(w-1)^{2n}, \quad n=0,1,\ldots \quad \text{(pion current)}. \quad (47)$$

This threshold "theorem" is a consequence of the positivity of a physical cross section combined with the crossing (9) in field theory. Experiments suggest that the current interacts predominantly with spin-$\frac{1}{2}$ fermions near $w=1$ in which case $F(w)$ is an odd function of $(w-1)$ near the threshold. Our crossing relation (9) then implies that this behavior can be continued to $w\lesssim 1$ and used to predict the annihilation process (1) in the proximity of $w=1$.

We want to emphasize that independent of the relative importance of $F_1(w)$ and $F_2(w)$ it follows from the existence of a Bjorken limit that the deep-inelastic annihilation cross section varies with total energy of the colliding electron-positron system as $1/q^2$ just the same as the cross section for a point hadron. Furthermore, even without calculating the specific values of $F_{1,2}(w)$ from a theory one can predict from (42) plus the observed structure functions for inelastic scattering that there will be a sizable cross section and many interesting channels to study in the deep inelastic region of colliding e^-e^+ beams.

The relative roles of the nucleon and pion currents can be studied experimentally by separating $F_1(w)$ from $F_2(w)$, or $\overline{W}_1$ from $\nu\overline{W}_2$ by the angular distribution in (42). The isotopic structure of the current can be studied by comparing the deep-inelastic cross sections leading to a detected proton or neutron.

(d) A parton model can also be formulated for deep-inelastic electron-meson scattering and electron-positron annihilation into a meson of fixed momentum plus "anything." The crossing properties of the two processes can also be established. For example, simple considerations show that for spin-0 mesons we have the substitution laws

$$\begin{aligned}\overline{W}_{\mu\nu}(q,P)&=W_{\mu\nu}(q,-P),\\ \overline{W}_1(q^2,\nu)&=W_1(q^2,-\nu),\\ \overline{W}_2(q^2,\nu)&=W_2(q^2,-\nu),\end{aligned} \quad (48)$$

where P_μ denotes the four-momentum of the meson in question; $W_{\mu\nu}$, $W_{1,2}$ and $\overline{W}_{\mu\nu}$, $\overline{W}_{1,2}$ are defined analo-

gously to those for nucleons. The sign difference between (48) and (5) comes about because pions are bosons and nucleons are fermions. In the Bjorken limit (48) gives

$$\begin{aligned}\bar{F}_1(w)&=+F_1(w),\\ \bar{F}_2(w)&=-F_2(w),\end{aligned}\tag{49}$$

where $F_{1,2}(w)$ and $\bar{F}_{1,2}(w)$ are defined by equations similar to (7)–(9). The threshold theorem for spin-0 mesons is

$$\begin{aligned}&F_2(w)=C_N'(w-1)^{2n}, \quad n=0,1,2,\ldots \\ &\qquad\qquad\qquad\qquad\text{(nucleon current)}\\ &F_2(w)=C_\pi'(w-1)^{2n+1}, \quad n=0,1,2,\ldots\\ &\qquad\qquad\qquad\qquad\text{(pion current)}.\end{aligned}\tag{50}$$

(e) By detecting different baryons in the final states, one has a simple test of the unitary symmetry scheme of strong interactions. For instance, according to SU_3 and the hypothesis that the electromagnetic current is a U-spin singlet, the differential cross sections labeled by the detected baryon and observed at identical values of q^2 and $q\cdot P$ should satisfy the relations

$$\begin{aligned}&\sigma_{\Xi^-}=\sigma_{\Sigma^-}, \quad \sigma_{\Sigma^+}=\sigma_p,\\ &\sigma_{\Xi^0}=\sigma_n=\tfrac{1}{2}(3\sigma_\Lambda-\sigma_{\Sigma^0}).\end{aligned}\tag{51}$$

Similar relations can be written for the mesons with an added constraint due to the fact that π^- and π^+ are each other's antiparticles; thus

$$\begin{aligned}&\sigma_{\pi^-}=\sigma_{K^-}=\sigma_{\pi^+}=\sigma_{K^+},\\ &\sigma_{K^0}=\sigma_{\bar{K}^0}=\tfrac{1}{2}(3\sigma_\eta-\sigma_{\pi^0}).\end{aligned}\tag{52}$$

This should be an ideal place to test the accuracy of SU_3 predictions since the mass differences among members of a multiplet should have a negligible effect on the dynamics as well as the kinematics in these regions of asymptotically large momentum and energy transfers.

(f) If charge conjugation is a good symmetry of the electromagnetic interactions, the differential cross sections for detecting a particle or its antiparticle are identical. According to (42), the differential cross section for (1) as a function of q^2 is comparable in magnitude to that for lepton-pair creation and very much larger than the observed "elastic" annihilation process to a $p\bar{p}$ pair. Consequently, it should be feasible by detecting and comparing charge-conjugate states, such as Λ and $\bar{\Lambda}$, for example, to test charge-conjugation conservation in electromagnetic interactions of hadrons.[8]

(g) One expects a large cross section for deep-inelastic electron-deuteron scattering, since the deuteron is a loosely bound system of a proton and a neutron and SLAC[5] data show a huge cross section for deep-inelastic electron-proton scattering. However, in the crossed channel of electron-positron annihilation to form a deuteron (or generally any other loosely bound "composite system" in place of the proton) plus anything else, the cross section should be very small. To see how this can be explained in the context of our results for scaling, consider explicitly deuteron production and note that the kinematically allowed regions are the same as illustrated in Fig. 1 but with the mass M now interpreted as the deuteron mass $M_d\approx 2M$. For inelastic scattering from the deuteron, the overwhelmingly large proportion of the cross section comes from the kinematic region corresponding to one of the nucleons in the deuteron serving as a spectator and the other as the target—i.e., for $w_d\equiv 2M_d\nu/Q^2>2$. When we probe into the region $1<w_d<2$ which is also kinematically allowed, we are simultaneously probing into very-large-momentum components of the deuteron wave function. To see this most directly we compute the invariant mass of the intermediate proton formed from the bound deuteron and moving in the infinite-momentum c.m. frame for the deuteron plus incident electron. The result, by a straightforward calculation with the kinematics shown in Fig. 6, is

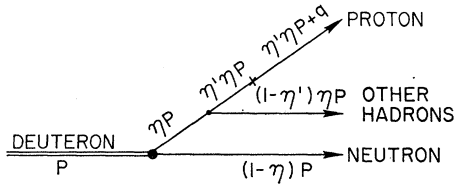

FIG. 6. Diagram for inelastic scattering from the deuteron. We suppress the transverse momenta in writing the labels for the kinematics as illustrated.

$$\mathfrak{M}^2-M^2\approx-\left(\frac{(w_d\eta'-2)^2}{w_d\eta'(w_d\eta'-1)}\right)M^2+\frac{4M\epsilon}{\eta' w_d},$$

where $0<\eta'<1$ is the fraction of longitudinal momentum of the intermediate proton retained on the final proton and $1-\eta'$ is the fraction acquired by all the other hadrons produced from the proton. This shows that only for $w_d=2/\eta'\geq 2$ are the low-momentum components of the deuteron contributing, so that the deuteron wave function does not severely damp the amplitudes νW_2 and W_1. In order to continue to the colliding-beam region as we did for proton targets, it would be necessary to continue across the boundary from $w_d>1$ to $w_d<1$. However, once w_d decreases below $w_d=2$, we have seen that the inelastic scattering is severely dampened; hence as we continue across the line $w_d=1$ into the annihilation region for $e^-e^+\to d+$"anything," we can expect the same very small cross section to be observed.

In contrast to this behavior, the deep-inelastic scattering cross section from a proton quickly grows to sizable values near $w=1$ and this in turn crosses to a large annihilation cross section. This difference reflects the qualitative difference between two systems—a loosely bound one such as the deuteron with mass approxi-

[8] If the baryon is built up of constituents or "partons" of spin 0 and $\frac{1}{2}$ only with minimal coupling to the electromagnetic fields as in our model, there is no possibility for C-violation asymmetries to appear due to the restraints imposed by current conservation alone.

mately equal to the sum of its constituents, and a tightly bound one such as the proton with mass substantially less than the sum of constituent masses, whatever they be. Historically the difference was often used to characterize "composite" versus "elementary" particles. We refrain here from such identification or labeling of systems, particularly since we have, as discussed earlier,[1] taken $Z_2=0$ so that the single "bare" proton state has zero probability of existing in the "physical" proton. Nevertheless, there remains a remnant of this view in our approach to the parton model. If we turn off the weak interactions, our final hadron multiparticle states in the Bjorken limit are composed of pions and nucleons appearing in (14) and (15), or the basic boson and fermion octets when we build in the SU_3 group. However, the higher resonances (vector mesons, the decuplet, etc.) are then composites built from these basic (or aristocratic) octet constituents, and whereas their *ratios* of cross sections for production in electron-positron annihilation may satisfy SU_3 predictions akin to (51) and (52), their magnitudes may be considerably smaller, similar to the deuteron's, since they are weakly bound or unstable. We have no basis for a firm prediction on these within our theoretical framework.

V. SUMMARY AND CONCLUSION

Under the same assumptions required in the study of deep-inelastic electron-nucleon scattering, we have accomplished the crossing to the annihilation channel and established the parton model for deep-inelastic electron-positron annihilation process (1). We found as an important consequence of this derivation that the deep-inelastic annihilation processes have very large cross sections and have the same energy dependence, at fixed $w\equiv 2M\nu/q^2$, as do the point-lepton cross sections. Moreover, these cross sections are orders of magnitude larger than the two-body process $e^-+e^+\to p+\bar{p}$. If verified, this result has important experimental implications since it suggests that there is a lot of interesting and observable physics to be done with colliding rings. Note that (42) integrates to

$$\Delta\sigma\approx\Delta w(4\pi\alpha^2/q^2)(\tfrac{1}{6}F_2-F_1)$$

in the interval Δw near $w=1$. Since $F_1\leq 0$ for $w<1$ according to (45), we take $\frac{1}{6}F_2-F_1>\frac{1}{6}F_2\sim\frac{1}{6}(\nu W_2)\sim 10^{-2}$ for $1.1<w<1.3$ as estimated from the scattering measurements. Independent of the ratio of F_1 to F_2 we can write near $w=1$, in terms of the separate contributions from the spin-0 bosons and spin-$\frac{1}{2}$ fermions, $F_2{}^B$ and $F_2{}^F$, respectively,

$$\tfrac{1}{6}F_2-F_1=\tfrac{1}{6}(F_2{}^B+2|F_2{}^F|)<\tfrac{1}{3}(\nu W_2) \quad \text{and} \quad >\tfrac{1}{6}(\nu W_2).$$

We thus arrive at a numerical prediction of

$$\sigma\sim(10^{-2}\Delta w)4\pi\alpha^2/q^2\approx 10^{-35}\ \text{cm}^2$$

for a colliding-beam total energy of $q=6$ GeV and $\Delta w\approx 0.2$. In contrast, for the two-body channel, the $p\bar{p}\to e\bar{e}$ annihilation measurements[9] put an upper limit of $\sigma\leq 5\times 10^{-34}$ cm^2 at a collision energy of $q=2.6$ GeV. The elastic cross section at high energy becomes

$$\sigma_{\text{el}}=\frac{4\pi\alpha^2}{q^2}\left[\tfrac{1}{3}|G_M(q^2)|^2+\frac{2}{3}\frac{M^2}{q^2}|G_E(q^2)|^2\right],$$

and may be as small as $\approx 2\times 10^{-39}$ cm^2 at $q=6$ GeV if $|G_M(36\ \text{GeV}^2)|^2\sim 10^{-6}$ as would follow from a simple dipole extrapolation of the elastic form factors.[10]

Finally, we note that here we do not have a sum rule for the structure functions analogous to that given in Eq. (82) of Paper II for inelastic scattering. In principle, therefore, the Bjorken limit for $\bar{W}_1$ and $\nu\bar{W}_2$ can be trivial since the structure functions might vanish in this limit. However, our dynamical relations between the structure functions W_1 and νW_2 for scattering and their continuations from the region $w>1$ to the annihilation region with $w<1$ as discussed in (43)–(47) indicate that this is not the case.

APPENDIX A

In this appendix we discuss the reasons preventing us from deriving the scaling laws for the structure functions of the annihilation problem in terms of current commutators as did Bjorken for the structure functions of the inelastic electron scattering. We want to show why we were driven to develop a canonical-field-theory model and a cumbersome time-ordered graphical analysis in order to accomplish the crossing to the annihilation channel.

For the inelastic electron scattering, the structure functions $W_1(q^2,\nu)$ and $W_2(q^2,\nu)$ are the absorptive parts of the spin-averaged forward Compton scattering amplitude for a spacelike virtual photon from a proton. Therefore they are given by the one-proton expectation value of the Fourier transform of the current commutator. Analyticity properties and asymptotic bounds of the scattering amplitude were utilized by Bjorken[2] in his derivation of the scaling laws for the structure functions in the inelastic electron scattering.

On the contrary, for the annihilation process (1) the structure functions $\bar{W}_1(q^2,\nu)$ and $\bar{W}_2(q^2,\nu)$ are not the absorptive parts of any scattering amplitude and as a result $\bar{W}_{\mu\nu}$ cannot be expressed as the matrix elements of a current commutator. To make this clear, consider the function $C_{\mu\nu}(q,P)$ defined by

$$C_{\mu\nu}(q,P)=4\pi^2\frac{E_p}{M}\int(dx)e^{iqx}\langle P|[J_\mu(x),J_\nu(0)]|P\rangle, \quad \text{(A1)}$$

where a spin average over the proton state is implied. $C_{\mu\nu}(q,P)$ as defined is the absorptive part of the forward Compton scattering of a photon with mass q^2

[9] Conversi *et al.*, Nuovo Cimento **40A**, 690 (1965); Hartell *et al.*, Stanford Linear Accelerator Report No. SLAC PUB-598, 1969 (unpublished).

[10] See W. K. H. Panofsky, in *Proceedings of the Fourteenth International Conference on High-Energy Physics, Vienna, 1968* (CERN, Geneva, 1968), p. 23.

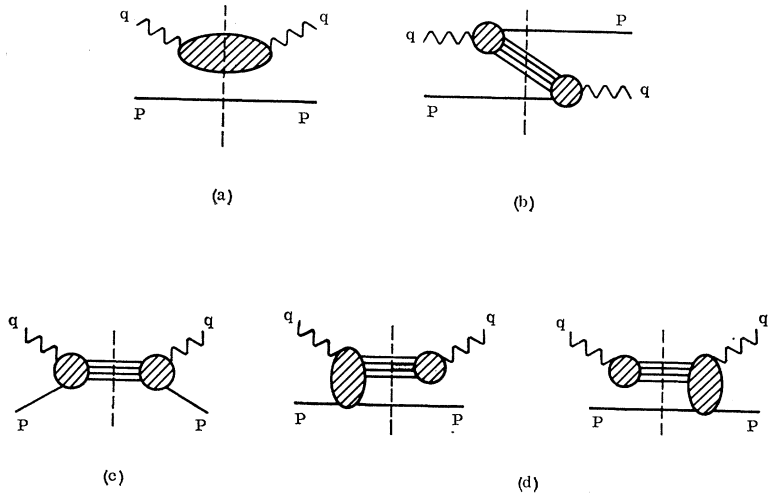

FIG. 7. General classes of diagrams contributing to the one-proton expectation value of the current commutator in the region of timelike q^2.

from a proton. For spacelike $q^2<0$ and $q^0>0$, only one ordering in the commutator contributes because of energy-momentum conservation and the stability of the proton. Thus we obtain, for spacelike q^2 and $q^0>0$,

$$C_{\mu\nu}(q,P)=4\pi^2\frac{E_p}{M}\int(dx)e^{iqx}\times\langle P|J_\mu(x)J_\nu(0)|P\rangle=W_{\mu\nu}(q,P), \quad \text{(A2)}$$

which shows that $W_{\mu\nu}(q,P)$ is given by the matrix elements of the current commutator. For timelike $q^2>0$ and $q^0>0$, however, $C_{\mu\nu}(q,P)$ contains contributions from several classes of diagrams with distinct connectedness properties. Let us write

$$C_{\mu\nu}(q,P)=C_{\mu\nu}^{(a)}(q,P)+C_{\mu\nu}^{(b)}(q,P)+C_{\mu\nu}^{(c)}(q,P)+C_{\mu\nu}^{(d)}(q,P), \quad \text{(A3)}$$

where the separate contributions $C_{\mu\nu}^{(a)},\ldots,C_{\mu\nu}^{(d)}$ are represented graphically in Fig. 7. Figure 7(a) represents the totally disconnected diagrams; Fig. 7(b) represents the correction to Fig. 7(a) demanded by the Pauli exclusion principle when the final states denoted by the blob in Fig. 7(a) contain protons; Fig. 7(c) represents the connected part; and Fig. 7(d) represents the semi-

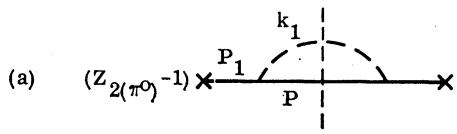

$P_1=\eta_1 P+k_{1\perp}$,
$k_1=(\eta_1-1)P+k_{1\perp}$, $k_{1\perp}\cdot P=0$
$Z_{2(\pi^0)}$ given by (18) of Paper II.

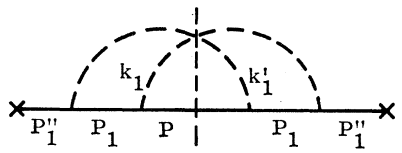

$P_1=\eta_1 P+k_{1\perp}$, $k_1=(\eta_1-1)P+k_{1\perp}$, $k_{1\perp}\cdot P=0$
$P_1'=\eta_1' P+k_{1\perp}'$, $k_1'=(\eta_1'-1)P+k_{1\perp}'$, $k_{1\perp}'\cdot P=0$
$P_1''=(\eta_1+\eta_1'-1)P+(k_{1\perp}+k_{1\perp}')$

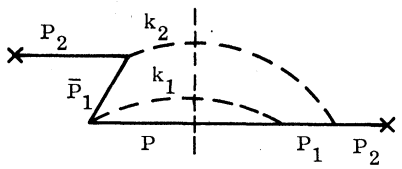

$P_1=\eta_1 P+k_{1\perp}=-\bar{P}_1$, $k_1=(\eta_1-1)P+k_{1\perp}$, $k_{1\perp}\cdot P=0$
$P_2=\eta_2 P_1+k_{2\perp}$, $k_2=(\eta_2-1)P_1+k_{2\perp}$, $k_{2\perp}\cdot P_1=0$

FIG. 8. Nucleon-current contributions to $\bar{W}_{\mu\nu}$ up to g^4 and the ladder diagram to any order.

(d)

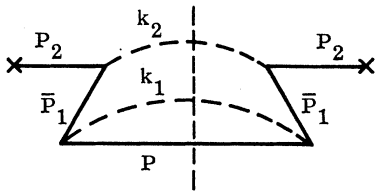

$\bar{P}_1 = -\eta_1 P - k_{1\perp} \equiv -P_1, \quad k_1 = (\eta_1 - 1)P + k_{1\perp}, \quad k_{1\perp} \cdot P = 0$

$P_2 = \eta_2 P_1 + k_{2\perp}, \quad k_2 = (\eta_2 - 1)P_1 + k_{2\perp}, \quad k_{2\perp} \cdot P_1 = 0$

(e)

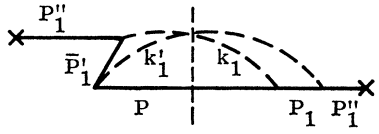

$P_1 = \eta_1 P + k_{1\perp}, \quad k_1 = (\eta_1 - 1)P + k_{1\perp}, \quad k_{1\perp} \cdot P = 0$

$\bar{P}'_1 = -\eta'_1 P - k'_{1\perp}, \quad k'_1 = (\eta'_1 - 1)P + k'_{1\perp}, \quad k'_{1\perp} \cdot P = 0$

$P''_1 = (\eta_1 + \eta'_1 - 1)P + (k_{1\perp} + k'_{1\perp})$

(f)

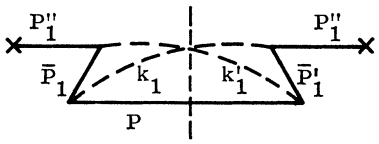

$\bar{P}_1 = -\eta_1 P - k_{1\perp}, \quad k_1 = (\eta_1 - 1)P + k_{1\perp}, \quad k_{1\perp} \cdot P = 0$

$\bar{P}'_1 = -\eta'_1 P - k'_{1\perp}, \quad k'_1 = (\eta'_1 - 1)P + k'_{1\perp}, \quad k'_{1\perp} \cdot P = 0$

$P''_1 = (\eta_1 + \eta'_1 - 1)P + (k_{1\perp} + k'_{1\perp})$

(g)

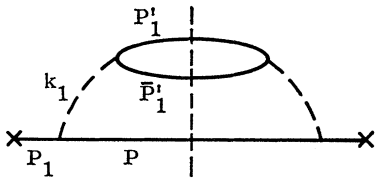

$P_1 = \eta_1 P + k_{1\perp}, \quad k_1 = (\eta_1 - 1)P + k_{1\perp}, \quad k_{1\perp} \cdot P = 0$

$P'_1 = \eta_2 k_1 + k_{2\perp}, \quad \bar{P}'_1 = (1 - \eta_2)k_1 - k_{2\perp}, \quad k_{2\perp} \cdot k_1 = 0$

(h)

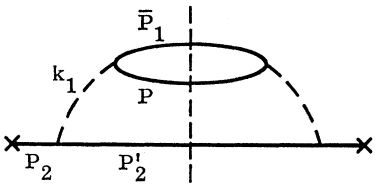

$\bar{P}_1 = -\eta_1 P - k_{1\perp}, \quad k_1 = (1 - \eta_1)P - k_{1\perp}, \quad k_{1\perp} \cdot P = 0$

$P_2 = \eta_2 k_1 + k_{2\perp}, \quad P'_2 = (\eta_2 - 1)k_1 + k_{2\perp}, \quad k_{2\perp} \cdot k_1 = 0$

FIG. 8 (*continued*)

disconnected diagrams arising from the interference between the two classes of diagrams in Figs. 7(a) and 7(c). Of special interest is the contribution from the class of diagrams in Fig. 7(b). It can be verified easily that

$$C_{\mu\nu}^{(b)}(q,P) = -\bar{W}_{\mu\nu}(q,P), \tag{A4}$$

where the minus sign is due to the Pauli exclusion principle, or Fermi statistics. In the physical region of the annihilation process (a), all the classes of diagrams in Fig. 7 are in principle nonvanishing. From (A3) and (A4) it is seen that $\bar{W}_{\mu\nu}(q,P)$ is *only a part* of the total absorptive part of the forward Compton scattering of a timelike virtual photon from a proton. Study of the current commutator, such as (A1) for timelike q^2, therefore, can only give insights to the sum of the pieces $C_{\mu\nu}^{(a)}, \ldots, C_{\mu\nu}^{(d)}$, not the object of interest $\bar{W}_{\mu\nu}(q,P)$ alone. Unless information about the pieces in (A3) other than $\bar{W}_{\mu\nu}(q,P)$ is known by other means, it can be concluded that study of the current commutator is not

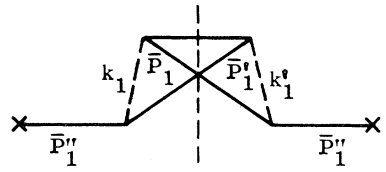

(i)

$\bar{P}_1 = -\eta_1 P - k_{1\perp}, \quad k_1 = (1-\eta_1)P - k_{1\perp}, \quad k_{1\perp}\cdot P = 0$

$\bar{P}'_1 = -\eta'_1 P - k'_{1\perp}, \quad k'_1 = (1-\eta'_1)P - k'_{1\perp}, \quad k'_{1\perp}\cdot P = 0$

$\bar{P}''_1 = (1-\eta_1-\eta'_1)P - (k_{1\perp}+k'_{1\perp})$

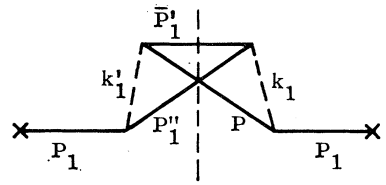

(j)

$P_1 = \eta_1 P + k_{1\perp}, \quad k_1 = (\eta_1-1)P + k_{1\perp}, \quad k_{1\perp}\cdot P = 0$

$\bar{P}'_1 = -\eta'_1 P - k'_{1\perp}, \quad k'_1 = (1-\eta'_1)P - k'_{1\perp}, \quad k'_{1\perp}\cdot P = 0$

$P''_1 = (\eta_1+\eta'_1-1)P + (k_{1\perp}+k'_{1\perp})$

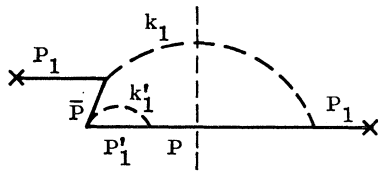

(k)

$P'_1 = \eta'_1 P + k'_{1\perp}, \quad k'_1 = (1-\eta'_1)P - k'_{1\perp}, \quad k'_{1\perp}\cdot P = 0$

$P_1 = \eta_1 P + k_{1\perp}, \quad k_1 = (1-\eta_1)P - k_{1\perp}, \quad k_{1\perp}\cdot P = 0$

$\bar{P} = -P$

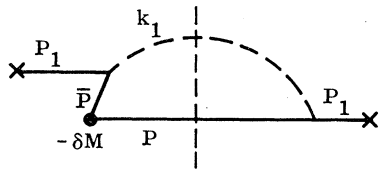

(l)

$\bar{P} = -P, \quad P_1 = \eta_1 P + k_{1\perp}, \quad k_1 = (\eta_1-1)P + k_{1\perp}, \quad k_{1\perp}\cdot P = 0$

δM given by (45) of Paper II.

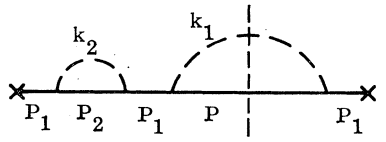

(m)

$P_1 = \eta_1 P + k_{1\perp}, \quad k_1 = (\eta_1-1)P + k_{1\perp}, \quad k_{1\perp}\cdot P = 0$

$P_2 = \eta_2 P_1 + k_{2\perp}, \quad k_2 = (1-\eta_2)P - k_{2\perp}, \quad k_{2\perp}\cdot P_1 = 0$

FIG. 8 (*continued*)

a useful approach to the understanding of the annihilation process (1).[11]

On the other hand, there is a one-to-one correspondence between individual Feynman amplitudes contributing to the inelastic electron-proton scattering and to the annihilation process (1). The crossing properties of field theory, or equivalently of individual Feynman amplitudes, relate the two by the subsitution law (5). Thus, canonical field theory provides a natural framework for going from the inelastic electron scattering to the electron-positron annihilation process (1). It is for this reason that we adopt the canonical field theory as a unified theoretical basis for describing both inelastic electron scattering and the electron-positron annihilation process (1).

As the development in this series of papers shows, a physical picture for both scattering and annihilation—the parton model—emerges from the field-theoretic study based on old-fashioned perturbation theory in the infinite-momentum frame. In our opionin, this picture sheds some light on the physical nature of the Bjorken limit and perhaps it may also lead to clues to a better understanding of purely hadronic processes at very high energies. We hold the point of view that despite its

[11] If one accepts Bjorken's "simple derivation" of scaling laws and uses the representation of the structure functions as sine transforms of almost equal-time current commutators, one concludes that $C_{\mu\nu}(q,P)=0$ for $0<w<1$. Further study utilizing this result is in progress by P. Roy and J. Pestieau (private communication).

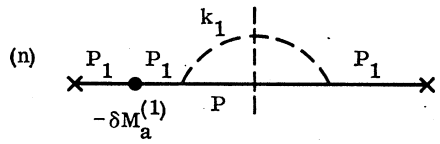

same parametrization as (a)

$\delta M_a^{(1)}$ given by (33) of Paper II.

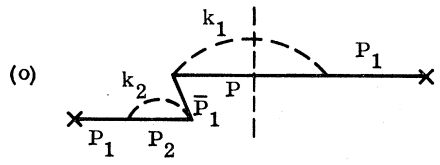

$P_1 = \eta_1 P + k_{1\perp} = -\bar{P}_1$, $k_1 = (\eta_1 - 1)P + k_{1\perp}$, $k_{1\perp} \cdot P = 0$

$P_2 = \eta_2 P_1 + k_{2\perp}$, $k_2 = (1-\eta_2)P_1 - k_{2\perp}$, $k_{2\perp} \cdot P_1 = 0$

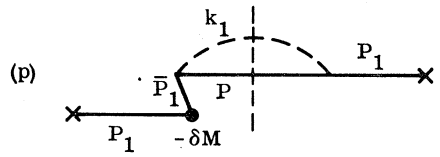

$P_1 = \eta_1 P + k_{1\perp}$, $k_1 = (\eta_1 - 1)P + k_{1\perp}$, $k_{1\perp} \cdot P = 0$

δM given by (45) of Paper II.

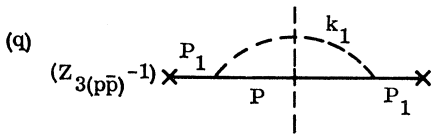

same parametrization as in (a)

$Z_{3(p\bar{p})}$ given by the $p\bar{p}$ contribution (Fig. 2b of II) to (20) of Paper II.

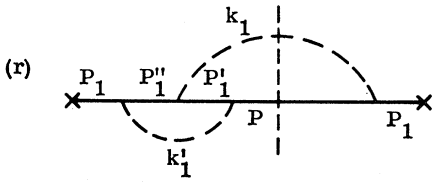

$P_1 = \eta_1 P + k_{1\perp}$, $k_1 = (\eta_1 - 1)P + k_{1\perp}$, $k_{1\perp} \cdot P = 0$

$P'_1 = \eta'_1 P + k'_{1\perp}$, $k'_1 = (1-\eta'_1)P - k'_{1\perp}$, $k'_{1\perp} \cdot P = 0$

$P''_1 = (\eta_1 + \eta'_1 - 1)P + (k_{1\perp} + k'_{1\perp})$

FIG. 8 (*continued*)

perennial disease of divergences encountered in a perturbation treatment, canonical field theory as the only self-contained formalism which embeds all the physical requirements of unitarity, crossing, relativity, etc., can be useful, when supplemented by *necessary* physical assumptions such as the transverse-momentum cutoff introduced in our analysis, as a guide to the general understanding of strong interactions.

APPENDIX B

In this appendix we explicitly verify the substitution law (9) in our field-theoretic model to fourth order in g for diagrams with nucleon-current contributions, and to any order for ladder diagrams with the nucleon current operating [Fig. 15 of Paper II and its corresponding diagram for annihilation process (1)]. We also present a few examples of pion-current contributions to fourth order for purpose of illustration. In the following, the detected nucleon is assumed to be a proton and all the pions are assumed to be neutral except the pion pair created by the current. Furthermore, only the results of $\bar{F}_2(w)$ will be given since $\bar{F}_1(w)$ is zero for a pion-current contribution and is related to $\bar{F}_2(w)$ by (40) for a nucleon-current contribution. In each diagram the momentum parametrization used in the calculation is given; $\bar{F}_2(w)^{(i)}$ denotes the contribution of Fig. 8(i) to $\bar{F}_2(w)$.

First we list the contributions in an obvious notation with a subscript relating them to the corresponding graphs in Figs. 8 and 9.

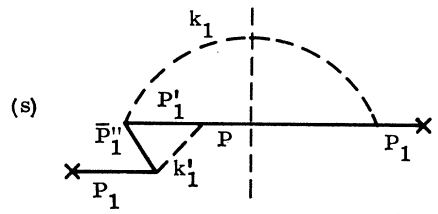

$P_1 = \eta_1 P + k_{1\perp}, \quad k_1 = (\eta_1 - 1)P + k_{1\perp}, \quad k_{1\perp} \cdot P = 0$

$P'_1 = \eta'_1 P + k'_{1\perp}, \quad k'_1 = (1-\eta'_1)P - k'_{1\perp}, \quad k'_{1\perp} \cdot P = 0$

$\bar{P}''_1 = (1 - \eta_1 - \eta'_1)P - (k_{1\perp} + k'_{1\perp})$

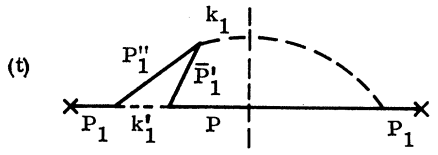

$P_1 = \eta_1 P + k_{1\perp}, \quad k_1 = (\eta_1 - 1)P + k_{1\perp}, \quad k_{1\perp} \cdot P = 0$

$\bar{P}'_1 = -\eta'_1 P - k'_{1\perp}, \quad k'_1 = (1-\eta'_1)P - k'_{1\perp}, \quad k'_{1\perp} \cdot P = 0$

$P''_1 = (\eta_1 + \eta'_1 - 1)P + (k_{1\perp}(k'_{1\perp})$

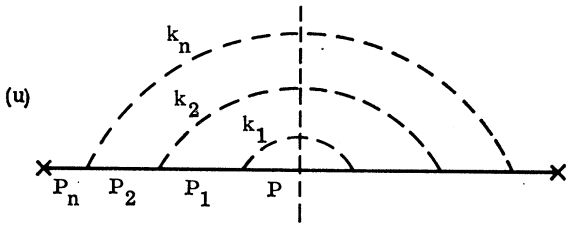

$P_i = \eta_i P_{i-1} + k_{i\perp}, \quad k_{i\perp} \cdot P_{i-1} = 0, \quad \eta_i > 1$

$k_i = (1-\eta_i)P_{i-1} - k_{i\perp}$

$i = 1, 2, \ldots n \quad (P_{i-1} \equiv P \text{ for } i=1)$

FIG. 8 (*continued*)

$$\bar{F}_2^{(8a)} = (Z_{2(\pi^0)} - 1)\frac{g^2}{16\pi^2}\frac{1}{w}\left(1 - \frac{1}{w}\right)\int dk_\perp^2 \frac{k_\perp^2 + M^2(1-1/w)^2}{[k_\perp^2 + M^2(1-1/w)^2 + \mu^2/w]^2},$$

$$\bar{F}_2^{(8b)} = (-)\left(\frac{g^2}{(2\pi)^3}\right)^2 M\nu \int \frac{d^3k_1}{2\omega_1}\frac{d^3k_1'}{2\omega_1'}\delta(q^2 - 2P_1'' \cdot q)\left(\frac{E_1''}{E_p}\right)^2$$

$$\times \frac{\mathrm{Tr}[(M-\gamma P)(M+\gamma P_1')(M-\gamma P_1'')(M+\gamma P_1)]}{(2E_1)(2E_1')(2E_1'')^2(E_p - E_1 + \omega_1)(E_p - E_1' + \omega_1')(E_p - E_1'' + \omega_1 + \omega_1')^2}$$

$$= \frac{1}{2}\left(\frac{g^2}{2(2\pi)^3}\right)^2 \frac{1}{w}\int d^2k_{1\perp} d^2k_{1\perp}' \int_{1/w}^1 \frac{d\eta_1}{\eta_1'}$$

$$\times \frac{\eta_1}{[k_{1\perp}^2 + M^2(1-\eta_1)^2 + \mu^2\eta_1][k_{1\perp}'^2 + M^2(1-\eta_1')^2 + \mu^2\eta_1']}$$

$$\times \frac{\begin{bmatrix} [k_{1\perp}'^2 + M^2(1-\eta_1')^2]\{[(1-\eta_1')k_{1\perp} + \eta_1 k_{1\perp}']^2 + M^2(1-\eta_1')^2\} \\ + [k_{1\perp}^2 + M^2(1-\eta_1)^2]\{[\eta_1' k_{1\perp} + (1-\eta_1)k_{1\perp}']^2 + M^2(1-\eta_1^2)^2\} \\ - [(k_{1\perp} + k_{1\perp}')^2 + M^2(2-\eta_1-\eta_1')^2][(\eta_1 k_{1\perp}' - \eta_1' k_{1\perp})^2 + M^2(\eta_1 - \eta_1')^2] \end{bmatrix}}{\begin{bmatrix} [(\eta_1 + \eta_1' - 1)/(1-\eta_1)][k_{1\perp}^2 + M^2(1-\eta_1)^2 + \mu^2\eta_1] \\ + [1/(1-\eta_1')][(k_{1\perp}(1-\eta_1') + k_{1\perp}'\eta_1)^2 + M^2(1-\eta_1')^2 + \mu^2\eta_1(\eta_1 + \eta_1' - 1)] \end{bmatrix}^2} \quad (\eta_1' = 1 - \eta_1 + 1/w),$$

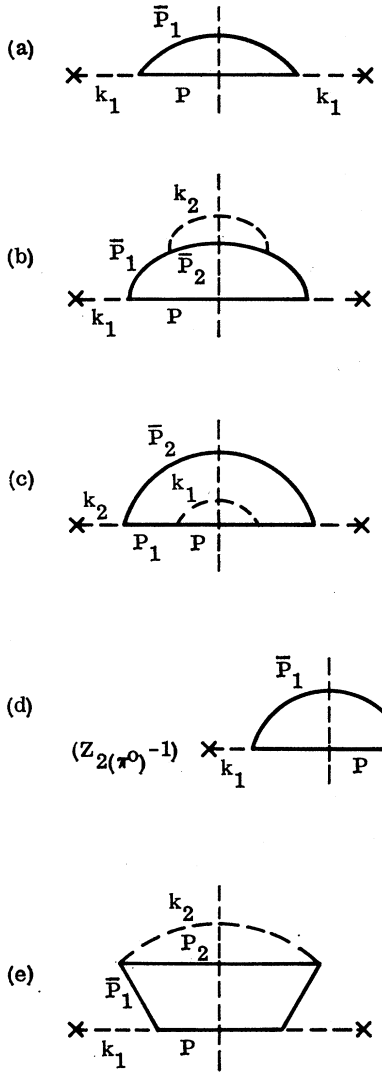

$\bar{P}_1 = -\eta_1 P + k_{1\perp}$, $k_1 = (1-\eta_1)P + k_{1\perp}$, $k_{1\perp}\cdot P = 0$

$\bar{P}_1 = -\eta_1 P + k_{1\perp}$, $k_1 = (1-\eta_1)P + k_{1\perp}$, $k_{1\perp}\cdot P = 0$
$\bar{P}_2 = \eta_2\bar{P}_1 + k_{2\perp}$, $k_2 = (1-\eta_2)\bar{P}_1 - k_{2\perp}$, $k_{2\perp}\cdot P = 0$

$P_1 = \eta_1 P + k_{1\perp}$, $k_1 = (\eta_1-1)P + k_{1\perp}$, $k_{1\perp}\cdot P = 0$
$\bar{P}_2 = -\eta_2 P_1 - k_{2\perp}$, $k_2 = (1-\eta_2)P_1 - k_{2\perp}$, $k_{2\perp}\cdot P_1 = 0$

same parametrization as in (a)

$Z_{2(\pi^0)}$ given by (18) of Paper II.

$\bar{P}_1 = +\eta_1 P - k_{1\perp} \equiv -P_1$, $k_1 = (1-\eta_1)P + k_{1\perp}$, $k_{1\perp}\cdot P = 0$
$P_2 = \eta_2 P_1 + k_{2\perp}$, $k_2 = (1-\eta_2)P_1 - k_{2\perp}$, $k_{2\perp}\cdot P_1 = 0$

FIG. 9. Typical examples of pion-current contributions up to g^4.

$$\bar{F}_2^{(8c)} = \left(\frac{g^2}{(2\pi)^3}\right)^2 M\nu \int \frac{d^3k_1}{2\omega_1}\frac{d^3k_2}{2\omega_2}\delta(q^2-2P_2\cdot q)\left(\frac{E_2}{E_p}\right)^2 \frac{\mathrm{Tr}[(M-\gamma P)(-M+\gamma\bar{P}_1)(M-\gamma P_2)(M+\gamma P_1)]}{(2E_1)(2\bar{E}_1)(2E_2)^2(E_p-E_1+\omega_1)(\bar{E}_1+E_2-\omega_2)(E_p-E_2+\omega_1+\omega_2)^2}$$

$$= \frac{1}{2}\left(\frac{g^2}{2(2\pi)^3}\right)^2 \frac{1}{w}\int d^2k_{1\perp}d^2k_{2\perp}\int_{1/w}^1 \frac{d\eta_1}{\eta_1}(1-\eta_2)$$

$$\times \frac{(k_{2\perp}+\eta_2 k_{1\perp})^2 + M^2(1-\eta_1\eta_2)^2 - \eta_2^2[k_{1\perp}^2+M^2(1-\eta_1)^2] - [k_{2\perp}^2+M^2(1-\eta_2)^2]}{[k_{1\perp}^2+M^2(1-\eta_1)^2+\mu^2\eta_1]\{[\eta_2(1-\eta_2)/(1-\eta_1)][k_{1\perp}^2+M^2(1-\eta_1)^2+\mu^2\eta_1]+k_{2\perp}^2+M^2(1-\eta_2)^2+\mu^2\eta_2\}^2}$$

$$(\eta_2 = 1/\eta_1 w),$$

$$\bar{F}_2^{(8d)} = \left(\frac{g^2}{(2\pi)^3}\right)^2 M\nu \int \frac{d^3k_1}{2\omega_1}\frac{d^3k_2}{2\omega_2}\delta(q^2-2P_2\cdot q)\left(\frac{E_2}{E_p}\right)^2 \frac{\mathrm{Tr}[(M-\gamma P)(M-\gamma\bar{P}_1)(M-\gamma P_2)(M-\gamma\bar{P}_1)]}{(2\bar{E}_1)^2(2E_2)^2(\bar{E}_1+E_2-\omega_2)^2(E_p-E_2+\omega_1+\omega_2)^2}$$

$$= \left(\frac{g^2}{2(2\pi)^3}\right)^2 \frac{1}{w^2}\int d^2k_{1\perp}d^2k_{2\perp}\int_{1/w}^1 \frac{d\eta_1}{\eta_1^3}\frac{1-\eta_2}{1-\eta_1}$$

$$\times \frac{1}{\{[\eta_2(1-\eta_2)/(1-\eta_1)][k_{1\perp}^2+M^2(1-\eta_1)^2+\mu^2\eta_1]+k_{2\perp}^2+M^2(1-\eta_2)^2+\mu^2\eta_2\}^2} \quad (\eta_2 = 1/\eta_1 w),$$

$$\bar{F}_2^{(8e)}=\left(\frac{g^2}{(2\pi)^3}\right)^2 M\nu\int\frac{d^3k_1}{2\omega_1}\frac{d^3k_1'}{2\omega_1'}\delta(q^2-2P_1''\cdot q)\left(\frac{E_1''}{E_p}\right)^2$$
$$\times\frac{\mathrm{Tr}[(M-\gamma P)(M-\gamma\bar{P}_1')(M-\gamma P_1'')(M+\gamma P_1)]}{(2E_1)(2\bar{E}_1')(2E_1'')^2(\bar{E}_1'+E_1''-\omega_1)(E_p-E_1''+\omega_1+\omega_1')^2(E_p-E_1+\omega_1)}$$

$$=(-)\frac{1}{2}\left(\frac{g^2}{2(2\pi)^3}\right)^2\frac{1}{w}\int d^2k_{1\perp}d^2k_{1\perp}'\int_{1/w}^1\frac{d\eta_1}{\eta_1'}\frac{\eta_1(1-\eta_1')}{k_{1\perp}^2+M^2(1-\eta_1)^2+\mu^2\eta_1}$$
$$\times\frac{\left[\begin{array}{r}[(1-\eta_1')k_{1\perp}+\eta_1k_{1\perp}']^2+M^2(1-\eta_1')^2-\eta_1^2[(k_{1\perp}+k_{1\perp}')^2\\ +M^2(2-\eta_1-\eta_1')^2]+(\eta_1+\eta_1'-1)^2[k_{1\perp}^2+M^2(1-\eta_1)^2]\end{array}\right]}{\left[\begin{array}{r}[(\eta_1+\eta_1'-1)(1-\eta_1')/(1-\eta_1)][k_{1\perp}^2+M^2(1-\eta_1)^2+\mu^2\eta_1]\\ +[k_{1\perp}(1-\eta_1)+k_{1\perp}'\eta_1]^2+M^2(1-\eta_1')^2+\mu^2\eta_1(\eta_1+\eta_1'-1)\end{array}\right]^2}\quad(\eta_1'=1-\eta_1+1/w),$$

$$\bar{F}_2^{(8f)}=(-)\left(\frac{g^2}{(2\pi)^3}\right)^2 M\nu\int\frac{d^3k_1}{2\omega_1}\frac{d^3k_1'}{2\omega_1'}\delta(q^2-2P_1''\cdot q)\left(\frac{E_1''}{E_p}\right)^2$$
$$\times\frac{\mathrm{Tr}[(M-\gamma P)(-M+\gamma\bar{P}_1')(M-\gamma P_1'')(-M+\gamma\bar{P}_1)]}{(2\bar{E}_1)(2\bar{E}_1')(\bar{E}_1'+E_1''-\omega_1)(\bar{E}_1+\bar{E}_1''-\omega_1')(E_p-E_1''+\omega_1+\omega_1')^2(2E''_1)^2}$$

$$=\left(\frac{g^2}{2(2\pi)^3}\right)^2\frac{1}{w^3}\int d^2k_{1\perp}d^2k_{1\perp}'\int_{1/w}^1\frac{d\eta_1}{\eta_1'}$$
$$\times\frac{\eta_1(1-\eta_1)(1-\eta_1')}{\left[\begin{array}{r}(1-\eta_1')(\eta_1+\eta_1'-1)[k_{1\perp}^2+M^2(1-\eta_1)^2+\mu^2\eta_1]\\ +(1-\eta_1)[(k_{1\perp}(1-\eta_1')+k_{1\perp}'\eta_1)^2+M^2(1-\eta_1')^2+\mu^2\eta_1(\eta_1+\eta_1'-1)]\end{array}\right]^2}\quad(\eta_1'=1-\eta_1+1/w),$$

$$\bar{F}_2^{(8g)}=(-)\left(\frac{g^2}{(2\pi)^3}\right)^2 M\nu\int\frac{d^3P_1'}{2E_1'}\frac{d^3\bar{P}_1'}{2\bar{E}_1'}\delta(q^2-2P_1\cdot q)\left(\frac{E_1}{E_p}\right)^2\frac{\mathrm{Tr}[(M-\gamma P)(M+\gamma P_1)]\,\mathrm{Tr}[(M-\gamma P_1')(-M+\gamma\bar{P}_1')]}{(2\omega_1)^2(2E_1)^2(E_2+\bar{E}_2-\omega_1)^2(E_p+E_2+\bar{E}_2-E_1)^2}$$

$$=2\left(\frac{g^2}{2(2\pi)^3}\right)^2\frac{1}{w}\left(1-\frac{1}{w}\right)\int d^2k_{1\perp}d^2k_{1\perp}'\int_0^1 d\eta_2$$
$$\times\frac{[k_{1\perp}^2+M^2(1-\eta_1)^2][k_{2\perp}^2+M^2]}{\{k_{1\perp}^2+M^2(1-\eta_1)^2+\mu^2\eta_1+[\eta_1/\eta_2(1-\eta_2)][k_{2\perp}^2+M^2-\mu^2\eta_2(1-\eta_2)]\}^2[k_{2\perp}^2+M^2-\mu^2\eta_2(1-\eta_2)]^2}$$
$$(\eta_1=1/w),$$

$$\bar{F}_2^{(8h)}=(-)\left(\frac{g^2}{(2\pi)^3}\right)^2 M\nu\int\frac{d^3\bar{P}_1}{2\bar{E}_1}\frac{d^3P_2'}{2E_2'}\delta(q^2-2P_2\cdot q)\left(\frac{E_2}{E_p}\right)^2\frac{\mathrm{Tr}[(M-\gamma P)(-M+\gamma\bar{P}_1)]\,\mathrm{Tr}[(M-\gamma P_2')(M+\gamma P_2)]}{(2\omega_1)^2(2E_2)^2(E_p+\bar{E}_1-\omega_1)^2(E_p+\bar{E}_1+E_2'-E_2)^2}$$

$$=2\left(\frac{g^2}{2(2\pi)^3}\right)^2\frac{1}{w^2}\int d^2k_{1\perp}d^2k_{2\perp}\int_{1/w}^1\frac{d\eta_2}{\eta_2}$$
$$\times\frac{\eta_1^2(k_{2\perp}^2+M^2)[k_{1\perp}^2+M^2(1-\eta_1)^2]}{[k_{1\perp}^2+M^2(1-\eta_1)^2+\mu^2\eta_1]^2\{\eta_2(1-\eta_2)[k_{1\perp}^2+M^2(1-\eta_1)^2+\mu^2\eta_1]+\eta_1[k_{2\perp}^2+M^2-\mu^2\eta_2(1-\eta_2)]\}^2}$$
$$(\eta_1=1-1/\eta_2w),$$

$$\bar{F}_2^{(8i)}=\left(\frac{g^2}{(2\pi)^3}\right)^2 M\nu\int\frac{d^3\bar{P}_1}{2\bar{E}_1}\frac{d^3\bar{P}_1'}{2\bar{E}_1'}\delta(q^2-2\bar{P}_1''\cdot q)\left(\frac{\bar{E}_1''}{E_p}\right)^2$$

$$\times\frac{\mathrm{Tr}[(M-\gamma P)(-M+\gamma\bar{P}_1)(-M-\gamma\bar{P}_1'')(-M+\gamma\bar{P}_1')]}{(2\omega_1)(2\omega_1')(2\bar{E}_1'')(E_p+\bar{E}_1-\omega_1)(E_p+\bar{E}_1'-\omega_1')(E_p+\bar{E}_1+\bar{E}_1'-\bar{E}_1'')^2}$$

$$=(-)\frac{1}{2}\left(\frac{g^2}{2(2\pi)^3}\right)^2\frac{1}{w}\int d^2k_{1\perp}d^2k_{1\perp}'\int_0^{1-1/w}\frac{d\eta_1}{\eta_1}\frac{\eta_1'(1-\eta_1)^2}{[k_{1\perp}^2+M^2(1-\eta_1)^2+\mu^2\eta_1][k_{1\perp}'^2+M^2(1-\eta_1')^2+\mu^2\eta_1']}$$

$$\times\frac{\left[\begin{array}{l}[k_{1\perp}'^2+M^2(1-\eta_1')^2]\{[(1-\eta_1')k_{1\perp}+\eta_1k_{1\perp}']^2+M^2(1-\eta_1')^2\}\\ \quad-[(\eta_1k_{1\perp}'-\eta_1'k_{1\perp})^2+M^2(\eta_1-\eta_1')^2][(k_{1\perp}+k_{1\perp}')^2+M^2(2-\eta_1-\eta_1')^2]\\ \quad+[k_{1\perp}^2+M^2(1-\eta_1)^2]\{[\eta_1'k_{1\perp}+(1-\eta_1)k_{1\perp}']^2+M^2(1-\eta_1^2)\}\end{array}\right]}{\left[\begin{array}{l}[\eta_1'(1-\eta_1-\eta_1')/\eta_1][k_{1\perp}^2+M^2(1-\eta_1)^2+\mu^2\eta_1]\\ \quad+[(1-\eta_1)k_{1\perp}'+\eta_1'k_{1\perp}]^2+M^2(1-\eta_1)^2-\mu^2\eta_1'(1-\eta_1-\eta_1')\end{array}\right]^2}\quad(\eta_1'=(1-\eta_1)-1/w),$$

$$\bar{F}_2^{(8j)}=\left(\frac{g^2}{(2\pi)^3}\right)^2 M\nu\int\frac{d^3k_1}{2\omega_1}\frac{d^3k_1'}{2\omega_1'}\delta(q^2-2P_1\cdot q)\left(\frac{E_1}{E_p}\right)^2$$

$$\times\frac{\mathrm{Tr}[(M-\gamma P)(-M+\gamma\bar{P}_1')(M-\gamma P_1'')(M+\gamma P_1)]}{(2\bar{E}_1')(2E_1'')(2E_1)^2(E_1''+\bar{E}_1'-\omega_1)(E_p+\bar{E}_1'-\omega_1')(E_p+\bar{E}_1'+E_1''-E_1)^2},$$

$$\bar{F}_2^{(8t)}=\left(\frac{g^2}{(2\pi)^3}\right)^2 M\nu\int\frac{d^3k_1}{2\omega_1}\frac{d^3k_1'}{2\omega_1'}\delta(q^2-2P_1\cdot q)\left(\frac{E_1}{E_p}\right)^2$$

$$\times\frac{\mathrm{Tr}[(M-\gamma P)(-M+\gamma\bar{P}_1')(M-\gamma P_1'')(M+\gamma P_1)]}{(2\bar{E}_1')(2E_1'')(\omega_1-\bar{E}_1'-E_1'')(E_p+\omega_1-E_1''-\omega_1')(2E_1)^2(E_p+\omega_1-E_1)^2}$$

$$=\bar{F}_2^{(8t_1)}+\bar{F}_2^{(8t_2)},\quad \eta_1+\eta_1'-1>0\ \text{ in }\ \bar{F}_2^{(8u_1)}\ \text{ and }\ \eta_1+\eta_1'-1<0\ \text{ in }\ \bar{F}_2^{(8u_2)},$$

$$\bar{F}_2^{(8j)}+\bar{F}_2^{(8t_1)}=\bar{F}_2^{(8j_1)}+\bar{F}_2^{(8j_2)}+\bar{F}_2^{(8j_3)}=(-)\left(\frac{g^2}{(2\pi)^3}\right)^2 M\nu\int\frac{d^3k_1}{2\omega_1}\frac{d^3k_1'}{2\omega_1'}\delta(q^2-2P_1\cdot q)\left(\frac{E_1}{E_p}\right)^2$$

$$\times\frac{\mathrm{Tr}[(M-\gamma\bar{P})(-M+\gamma\bar{P}_1')(M-\gamma P_1'')(M+\gamma P_1)]}{(2\bar{E}_1')(2E_1'')(2E_1)^2}\left[\frac{1}{(E_p+\bar{E}_1'-\omega_1')(E_p+\bar{E}_1'+E_1''-E_1)(E_p+\omega_1-E_1)^2}\right.$$

$$\left.+\frac{1}{(E_p+\bar{E}_1'-\omega_1')(E_p+\bar{E}_1'+E_1''-E_1)^2(E_p+\omega_1-E_1)}+\frac{1}{(E_p+\omega_1-E_1''-\omega_1')(E_p+\bar{E}_1'-\omega_1')(E_p+\omega_1-E_1)^2}\right],$$

$$\bar{F}_2^{(8j_1)}=(-)\frac{1}{2}\left(\frac{g^2}{2(2\pi)^3}\right)^2\frac{1}{w}\left(1-\frac{1}{w}\right)^2\int d^2k_{1\perp}d^2k_{1\perp}'\int_0^{1-1/w}\frac{d\eta_1'}{1-\eta_1-\eta_1'}$$

$$\times\frac{1}{[k_{1\perp}'^2+M^2(1-\eta_1')^2+\mu^2\eta_1'][k_{1\perp}^2+M^2(1-\eta_1)^2+\mu^2\eta_1]^2}$$

$$\times\frac{1}{[\eta_1'(1-\eta_1-\eta_1')/\eta_1][k_{1\perp}^2+M^2(1-\eta_1)^2+\mu^2\eta_1]+\{[(1-\eta_1)k_{1\perp}'+\eta_1'k_{1\perp}]^2+M^2(1-\eta_1)^2-\mu^2\eta_1'(1-\eta_1-\eta_1')\}}$$

$$\times\{[k_{1\perp}'^2+M^2(1-\eta_1')^2][((1-\eta_1')k_{1\perp}+\eta_1k_{1\perp}')^2+M^2(1-\eta_1')^2]-[(\eta_1k_{1\perp}'-\eta_1'k_{1\perp})^2+M^2(\eta_1-\eta_1')^2]$$

$$\times[(k_{1\perp}+k_{1\perp}')^2+M^2(2-\eta_1-\eta_1')^2]+[k_{1\perp}^2+M^2(1-\eta_1)^2][(\eta_1'k_{1\perp}+(1-\eta_1)k'_{1\perp})^2+M^2(1-\eta_1)^2]\}$$

$$(\eta_1=1/w),$$

$$\bar{F}_2^{(8j_2)}=(-)\frac{1}{2}\left(\frac{g^2}{2(2\pi)^3}\right)^2\left(1-\frac{1}{w}\right)^2\int d^2k_{1\perp}d^2k_{1\perp}'\int_0^{1-1/w}d\eta_1'\eta_1'\frac{1}{[k_{1\perp}'^2+M^2(1-\eta_1')^2+\mu^2\eta_1'][k_{1\perp}^2+M^2(1-\eta_1)^2+\mu^2\eta_1]}$$

$$\times\frac{\left[\begin{array}{l}[k_{1\perp}'^2+M^2(1-\eta_1')^2]\{[(1-\eta_1')k_{1\perp}+\eta_1k_{1\perp}']^2+M^2(1-\eta_1')^2\}\\ \quad-[(\eta_1k_{1\perp}'-\eta_1'k_{1\perp})^2+M^2(\eta_1-\eta_1')^2][(k_{1\perp}+{}_{1\perp}')^2+M^2(2-\eta_1-\eta_1')^2]\\ \quad+[k_{1\perp}^2+M^2(1-\eta_1)^2]\{[\eta_1'k_{1\perp}+(1-\eta_1)k_{1\perp}']^2+M^2(1-\eta_1)^2\}\end{array}\right]}{\left[\begin{array}{l}[\eta_1'(1-\eta_1-\eta_1')/\eta_1][k_{1\perp}^2+M^2(1-\eta_1)^2+\mu^2\eta_1]+[(1-\eta_1)k_{1\perp}'+\eta_1'k_{1\perp}]^2\\ \quad+M^2(1-\eta_1)^2-\mu^2\eta_1'(1-\eta_1-\eta_1')^2\end{array}\right]}\quad(\eta_1=1/w),$$

$$\bar{F}_2^{(8j_3)}=\frac{1}{2}\left(\frac{g^2}{2(2\pi)^3}\right)^2\frac{1}{w^2}\left(1-\frac{1}{w}\right)\int d^2k_{1\perp}d^2k_{1\perp}'\int_{1-1/w}^0 d\eta'$$

$$\times\frac{1}{\eta_1'(\eta_1+\eta_1'-1)[k_{1\perp}'^2+M^2(1-\eta_1')^2+\mu^2\eta_1'][k_{1\perp}^2+M^2(1-\eta_1)^2+\mu^2\eta_1]^2}$$

$$\times\frac{1}{\left[\begin{array}{l}[(\eta_1+\eta_1'-1)/(1-\eta_1)][k_{1\perp}^2+M^2(1-\eta_1)^2+\mu^2\eta_1]+[1/(1-\eta_1')]\\ \quad\times\{[k_{1\perp}(1-\eta_1')+k_{1\perp}'\eta_1]^2+M^2(1-\eta_1')^2+\mu^2\eta_1(\eta_1+\eta_1'-1)\}\end{array}\right]}$$

$$\times\{[k_{1\perp}'^2+M^2(1-\eta_1')^2][((1-\eta_1')k_{1\perp}+\eta_1k_{1\perp}')^2+M^2(1-\eta_1')^2]-[(k_{1\perp}+k_{1\perp}')^2$$

$$+M^2(2-\eta_1-\eta_1')^2][(\eta_1k_{1\perp}'-\eta_1'k_{1\perp})^2+M^2(\eta_1-\eta_1')^2]+[k_{1\perp}^2+M^2(1-\eta_1)^2]$$

$$\times[((1-\eta_1)k_{1\perp}'+\eta_1'k_{1\perp})^2+M^2(1-\eta_1)^2]\}\quad(\eta_1=1/w),$$

$$F_2^{(8t_2)}=(-)\frac{1}{2}\left(\frac{g^2}{2(2\pi)^3}\right)^2\frac{1}{w^2}\left(1-\frac{1}{w}\right)\int d^2k_{1\perp}d^2k_{1\perp}'\int_0^1 d\eta_1'\frac{1}{\eta_1'(\eta_1+\eta_1'-1)}\frac{1}{[k_{1\perp}^2+M^2(1-\eta_1)^2+\mu^2\eta_1]^2}$$

$$\times\frac{\left[\begin{array}{l}[(1-\eta_1')k_{1\perp}+\eta_1k_{1\perp}']^2+M^2(1-\eta_1')^2-\eta_1^2[(k_{1\perp}+k_{1\perp}')^2+M^2(2-\eta_1-\eta_1')^2]\\ \quad+(\eta_1+\eta_1'-1)^2[k_{1\perp}^2+M^2(1-\eta_1)^2]\end{array}\right]}{\left[\begin{array}{l}[(1-\eta_1')/(1-\eta_1)](\eta_1+\eta_1'-1)[k_{1\perp}^2+M^2(1-\eta_1)^2+\mu^2\eta_1]+[(1-\eta_1')k_{1\perp}+\eta_1k_{1\perp}']^2\\ \quad+M^2(1-\eta_1')^2+\mu^2\eta_1(\eta_1+\eta_1'-1)\end{array}\right]}\quad(\eta_1=1/w),$$

$$\bar{F}_2^{(8k)}=(-)\left(\frac{g^2}{(2\pi)^3}\right)^2M\nu\int\frac{d^3k_1}{2\omega_1}\frac{d^3k_1'}{2\omega_1'}\delta(q^2-2P_1\cdot q)\left(\frac{E_1}{E_p}\right)^2$$

$$\times\frac{\mathrm{Tr}[(M-\gamma P_1')(-M+\gamma\bar{P})(M-\gamma P_1)(M+\gamma P)]}{(2E_1')(2\bar{E})(2E_1)^2(E_p-\omega_1'-E_1')(E_p+\omega_1-E_1-\bar{E}-\omega_1'-E_1')(E_p+\omega_1-E_1)^2}$$

$$=(-)\left(\frac{g^2}{2(2\pi)^3}\right)^2\frac{1}{w}\left(1-\frac{1}{w}\right)\frac{1}{2}\int d^2k_{1\perp}d^2k_{1\perp}'\int_0^1\frac{d\eta_1'}{\eta_1'}\frac{1}{[k_{1\perp}'^2+M^2(1-\eta_1')^2+\mu^2\eta_1'][k_{1\perp}^2+M^2(1-\eta_1)^2+\mu^2\eta_1]^2}$$

$$\times\{\eta_1^2[k_{1\perp}'^2+M^2(1-\eta_1')^2]-[(\eta_1k_{1\perp}'-\eta_1'k_{1\perp})^2+M^2(\eta_1-\eta_1')^2]+\eta_1'^2[k_{1\perp}^2+M^2(1-\eta_1)^2]\}\quad(\eta_1=1/w),$$

$$\bar{F}_2^{(1)}=\left(\frac{g^2}{(2\pi)^3}\right)\delta M(M\nu)\int\frac{d^3k_1}{2\omega_1}\delta(q^2-2P_1\cdot q)\left(\frac{E_1}{E_p}\right)^2\frac{\mathrm{Tr}[(M-\gamma P)(M+\gamma\bar{P})(M+\gamma P_1)]}{(2\bar{E})(-\bar{E}-E_1+\omega_1)(E_p-E_1+\omega_1)^2(2E_1)^2}$$

$$=\left(\frac{g^2}{2(2\pi)^3}\right)M\delta M\frac{1}{w^2}\left(1-\frac{1}{w}\right)^2\int d^2k_{1\perp}\frac{1}{[k_{1\perp}^2+M^2(1-1/w)^2+\mu^21/w]^2},$$

$$\bar{F}_2^{(8m)}+\bar{F}_2^{(8n)}=\left(\frac{g^2}{2(2\pi)^3}\right)^2\int\frac{d^3k_1}{\omega_1}\frac{d^3k_2}{\omega_2}\delta\left(\eta_1-\frac{1}{w}\right)\left(\frac{E_1}{E_p}\right)^2$$
$$\times\frac{4(M^2-P\cdot P_1)(M^2-P_1\cdot P_2)}{(2E_1)^2(E_p-E_1+\omega_1)^2(2E_1)(E_1-E_2-\omega_2)2E_2(E_p-E_2+\omega_1-\omega_2)}$$
$$=(-)\left(\frac{g^2}{2(2\pi)^3}\right)^2\frac{1}{w}\left(1-\frac{1}{w}\right)\int d^2k_{1\perp}d^2k_{2\perp}\int_0^1 d\eta_2(1-\eta_2)$$
$$\times\frac{[k_{1\perp}^2+M^2(1-\eta_1)^2][k_{2\perp}^2+M^2(1-\eta_2)^2]}{\left[\begin{array}{l}[k_{1\perp}^2+M^2(1-\eta_1)^2+\mu^2\eta_1]^2[k_{2\perp}^2+M^2(1-\eta_2)^2+\mu^2\eta_2]\\ \quad\times\{[\eta_2(1-\eta_2)/(1-\eta_1)][k_{1\perp}^2+M^2(1-\eta_1)^2+\mu^2\eta_1]+k_{2\perp}^2+M^2(1-\eta_2)^2+\mu^2\eta_2\}\end{array}\right]}\quad(\eta_1=1/w),$$

$$\bar{F}_2^{(8o)}=\frac{1}{2}\left(\frac{g^2}{2(2\pi)^3}\right)^2\int\frac{d^3k_1}{\omega_1}\frac{d^3k_2}{\omega_2}\delta\left(\eta_1-\frac{1}{w}\right)\left(\frac{E_1}{E_p}\right)^2$$
$$\times\frac{4[(M^2-P\cdot P_1)(M^2+\bar{P}_1\cdot P_2)-(M^2-P\cdot P_2)(M^2+P_1\cdot\bar{P}_1)+(M^2+P\cdot\bar{P}_1)(M^2-P_1\cdot P_2)]}{(2E_2)(E_p-E_1+\omega_1)^2 2\bar{E}_1(E_1+E_2+\omega_2)(2E_1)^2(E_p-E_2+\omega_1-\omega_2)}$$
$$=\frac{1}{2}\left(\frac{g^2}{2(2\pi)^3}\right)^2\frac{1}{w}\left(1-\frac{1}{w}\right)\int d^2k_{1\perp}d^2k_{2\perp}\int_0^1\frac{d\eta_2}{\eta_2}$$
$$\times\frac{[(k_{2\perp}+\eta_2k_{1\perp})^2+M^2(1-\eta_1\eta_2)^2]-\eta_2^2[k_{1\perp}^2+M^2(1-\eta_1)^2]-[k_{2\perp}^2+M^2(1-\eta_2)^2]}{\left[\begin{array}{l}[k_{1\perp}^2+M^2(1-\eta_1)^2+\mu^2\eta_1]^2\{[\eta_2(1-\eta_2)/(1-\eta_1)]\\ \quad\times[k_{1\perp}^2+M^2(1-\eta_1)^2+\mu^2\eta_1]+k_{2\perp}^2+M^2(1-\eta_2)^2+\mu^2\eta_2\}\end{array}\right]}\quad(\eta_1=1/w),$$

$$\bar{F}_2^{(8p)}=(-)\left(\frac{g^2}{(2\pi)^3}\right)\delta M(M\nu)\int\frac{d^3k_1}{2\omega_1}\delta(q^2-2P_1\cdot q)\left(\frac{E_1}{E_p}\right)^2\frac{\mathrm{Tr}[(M+\gamma P)(M+\gamma\bar{P}_1)(M-\gamma P_1)]}{(2\bar{E}_1)(2E_1)^2(-E_1-\bar{E}_1)(E_p-E_1+\omega_1)^2}$$
$$=-\left(\frac{g^2}{2(2\pi)^3}\right)\delta MM\frac{1}{w}\left(1-\frac{1}{w}\right)^2\int d^2k_{1\perp}\frac{1}{[k_{1\perp}^2+M^2(1-1/w)^2+\mu^2/w]^2},$$

$$\bar{F}_2^{(8q)}=(Z_{3(p\bar{p})}-1)\bar{F}_2^{(8a)},$$

$$\bar{F}_2^{(8r)}=(-)\left(\frac{g^2}{2(2\pi)^3}\right)^2M\nu\int\frac{d^3k_1}{\omega_1}\frac{d^3k_1'}{\omega_1'}\delta(q^2-2P_1\cdot q)\left(\frac{E_1}{E_p}\right)^2$$
$$\times\frac{\mathrm{Tr}[(M-\gamma P)(M+\gamma P_1')(M-\gamma P_1'')(M+\gamma P_1)]}{(2E_1')(2E_1'')(E_p-E_1'-\omega_1')(E_p-E_1''+\omega_1-\omega_1')(2E_1)^2(E_p-E_1+\omega_1)^2},$$

$$\bar{F}_2^{(8r)}=\bar{F}_2^{(8r_1)}+\bar{F}_2^{(8r_2)},$$

$$\bar{F}_2^{(8r_1)}=\frac{1}{2}\left(\frac{g^2}{2(2\pi)^3}\right)^2\frac{1}{w^2}\left(1-\frac{1}{w}\right)\int d^2k_{1\perp}d^2k_{1\perp}'\int_0^1 d\eta'$$
$$\times\frac{1}{\eta_1'(\eta_1+\eta_1'-1)[k_{1\perp}'^2+M^2(1-\eta_1')^2+\mu^2\eta_1'][k_{1\perp}^2+M^2(1-\eta_1)^2+\mu^2\eta_1]^2}$$
$$\times\frac{1}{\left[\begin{array}{l}[(\eta_1+\eta_1'-1)/(1-\eta_1)][k_{1\perp}^2+M^2(1-\eta_1)^2+\mu^2\eta_1]+[1/(1-\eta_1')]\\ \quad\times\{[k_{1\perp}(1-\eta_1')+k_{1\perp}'\eta_1]^2+M^2(1-\eta_1')^2+\mu^2\eta_1(\eta_1+\eta_1'-1)\}\end{array}\right]}$$
$$\times\{[k_{1\perp}'^2+M^2(1-\eta_1')^2][((1-\eta_1')k_{1\perp}+\eta_1k_{1\perp}')^2+M^2(1-\eta_1')^2]-[(k_{1\perp}+k_{1\perp}')^2+M^2(2-\eta_1-\eta_1')^2]$$
$$\times[(\eta_1k_{1\perp}'-\eta_1'k_{1\perp})^2+M^2(\eta_1-\eta_1')^2]+[k_{1\perp}^2+M^2(1-\eta_1)^2][((1-\eta_1)k_{1\perp}'+\eta_1'k_{1\perp})^2+M^2(1-\eta_1)^2]\}$$
$$(\eta_1=1/w),$$

$$\bar{F}_2^{(8r_2)}=(-)\frac{1}{2}\left(\frac{g^2}{2(2\pi)^3}\right)^2\frac{1}{w^2}\left(1-\frac{1}{w}\right)\int d^2k_{1\perp}d^2k_{1\perp}'\int_{1-1/w}^{1}d\eta_1'\frac{1}{\eta_1'(\eta_1+\eta_1'-1)}\frac{1}{[k_{1\perp}^2+M^2(1-\eta_1)^2+\mu^2\eta_1]^2}$$

$$\times\frac{\left[\begin{array}{r}[(1-\eta_1')k_{1\perp}+\eta_1k_{1\perp}']^2+M^2(1-\eta_1')^2-\eta_1^2[(k_{1\perp}+k_{1\perp}')^2+M^2(2-\eta_1-\eta_1')^2]\\+(\eta_1+\eta_1'-1)^2[k_{1\perp}^2+M^2(1-\eta_1)^2]\end{array}\right]}{\left[\begin{array}{r}[(1-\eta_1')/(1-\eta_1)](\eta_1+\eta_1'-1)[k_{1\perp}^2+M^2(1-\eta_1)^2+\mu^2\eta_1]+[(1-\eta_1')k_{1\perp}+\eta_1k_{1\perp}']^2\\+M^2(1-\eta_1')^2+\mu^2\eta_1(\eta_1+\eta_1'-1)\end{array}\right]}\quad(\eta_1=1/w),$$

$$\bar{F}_2^{(8s)}=\left(\frac{g^2}{2(2\pi)^3}\right)^2M\nu\int\frac{d^3k_1}{2\omega_1}\frac{d^3k_1'}{2\omega_1'}\delta(q^2-2P_1\cdot q)\left(\frac{E_1}{E_p}\right)^2$$

$$\times\frac{\mathrm{Tr}[(M-\gamma P)(M+\gamma P_1')(-M-\gamma\bar{P}_1'')(M+\gamma P_1)]}{(2E_1')(2\bar{E}_1'')(E_p-E_1'-\omega_1')(E_p-E_1'-\bar{E}_1''-E_1)(E_p-E_1+\omega_1)^2(2E_1)^2}$$

$$=(-)\frac{1}{2}\left(\frac{g^2}{2(2\pi)^3}\right)^2\frac{1}{w}\left(1-\frac{1}{w}\right)\int d^2k_{1\perp}d^2k_{1\perp}'\int_0^1d\eta_1'\frac{1}{\eta_1'(\eta_1+\eta_1'-1)}$$

$$\times\frac{\eta_1^2[k_{1\perp}'^2+M^2(1-\eta_1')^2]-[(\eta_1k_{1\perp}'-\eta_1'k_{1\perp})^2+M^2(\eta_1-\eta_1')^2]+\eta_1'^2[k_{1\perp}^2+M^2(1-\eta_1)^2]}{[k_{1\perp}'^2+M^2(1-\eta_1')^2+\mu^2\eta_1'][k_{1\perp}^2+M^2(1-\eta_1)^2+\mu^2\eta_1]^2}\quad(\eta_1=1/w),$$

$$\bar{F}_2^{(8u)_{[n\pi^0]}}=(-)\left(\frac{g^2}{(2\pi)^3}\right)^nM\nu\int\prod_{i=1}^{n}\frac{d^3k_i}{2\omega_i}\delta(q^2-2P_n\cdot q)\left(\frac{E_n}{E_p}\right)^2$$

$$\times\frac{\mathrm{Tr}[(M+\gamma P)\gamma_5(M+\gamma P_1)(M+\gamma P_{n-1})\gamma_5(M+\gamma P_n)\gamma_5(M+\gamma P_{n-1})\cdots\gamma_5(M+\gamma P_1)\gamma_5]}{(2E_1)^2\cdots(2E_n)^2(E_p-E_1+\omega_1)^2\cdots(E_p-E_n+\omega_1+\cdots+\omega_n)^2}$$

$$=\left(\frac{g^2}{2(2\pi)^3}\right)^n\int\prod_{i=1}^{n}d^2k_{i\perp}\int_{1/w}^{1}\frac{d\eta_1}{\eta_1}\cdots\int^{1}\frac{1}{\eta_1\cdots\eta_{n-2}w}\frac{d\eta_{n-1}}{\eta_{n-1}}$$

$$\times\left\{\frac{(1-\eta_1)\cdots(1-\eta_n)[k_{1\perp}^2+M^2(1-\eta_1)^2]\cdots[k_{n\perp}^2+M^2(1-\eta_n)^2]}{[k_{1\perp}^2+M^2(1-\eta_1)^2+\mu^2\eta_1]^2\{[\eta_2(1-\eta_2)/(1-\eta_1)][k_{1\perp}^2+M^2(1-\eta_1)^2+\mu^2\eta_1]+[k_{2\perp}^2+M^2(1-\eta_2)^2+\mu^2\eta_2]\}^2}\right.$$

$$\left.\times\cdots\frac{1}{\{[\eta_2\cdots\eta_n(1-\eta_n)/(1-\eta_1)][k_{1\perp}^2+M^2(1-\eta_1)^2+\mu^2\eta_1]+\cdots+[k_{n\perp}^2+M^2(1-\eta_n)^2+\mu^2\eta_n]\}^2}\right\}$$

$$(\eta_1\cdots\eta_n=1/w),$$

$$\bar{F}_2^{(9a)}=\frac{g^2}{8\pi^2}\frac{1}{w^2}\int dk_{1\perp}^2\frac{k_\perp^2+M^2/w^2}{[k_{1\perp}^2+M^2/w^2+\mu^2(1-1/w)]^2},$$

$$\bar{F}_2^{(9b)}=(-)\left(\frac{g^2}{(2\pi)^3}\right)^2M\nu\int\frac{d^3\bar{P}_2}{2\bar{E}_2}\frac{d^3k_2}{2\omega_2}\delta(q^2-2k_1\cdot q)\left(\frac{\omega_1}{E_p}\right)^2\frac{\mathrm{Tr}[(M-\gamma P)(M-\gamma\bar{P}_1)(M+\gamma\bar{P}_2)(M-\gamma\bar{P}_1)]}{(2\bar{E}_1)^2(2\bar{E})^2(E_2+\omega_2-\bar{E}_1)^2(E_p+\bar{E}_2+\omega_2-\omega_1)^2}$$

$$=2\left(\frac{g^2}{16\pi^2}\right)^2\frac{1}{w^3}\int dk_{1\perp}^2dk_{2\perp}^2\int_0^1d\eta_2$$

$$\times\frac{(1-\eta_2)[k_{1\perp}^2+M^2(1-\eta_1)^2][k_{2\perp}^2+M^2(1-\eta_2)^2]}{\left[\begin{array}{r}[k_{2\perp}^2+M^2(1-\eta_2)^2+\mu^2\eta_2]^2\{k_{1\perp}^2+M^2(1-\eta_1)^2+\mu^2\eta_1\\+[(1-\eta_1)/\eta_2(1-\eta_2)][k_{2\perp}^2+M^2(1-\eta_2)^2+\mu^2\eta_2]\}^2\end{array}\right]}\quad(\eta_1=1-1/w),$$

$$\bar{F}^{c(9c)}=(-)\left(\frac{g^2}{(2\pi)^3}\right)^2 2M\nu\int\frac{d^3k_1}{2\omega_1}\frac{d^3\bar{P}_1}{2\bar{E}_2}\delta(q^2-2k_2\cdot q)\left(\frac{\omega_2}{E_p}\right)^2\frac{\mathrm{Tr}[(M-\gamma P)(M+\gamma P_1)(M+\gamma\bar{P}_2)(M+\gamma P_1)]}{(2E_1)^2(2\omega_2)^2(E_p-E_1+\omega_1)^2(E_p+\bar{E}_2+\omega_1-\omega_2)^2}$$

$$=2\left(\frac{g^2}{2(2\pi)^2}\right)^2\frac{1}{w^2}\int d^2k_{1\perp}d^2k_{2\perp}\int_{1/w}^1\frac{d\eta_1}{\eta_1}(1-\eta_1)^3$$

$$\times\frac{[k_{1\perp}^2+M^2(1-\eta_1)^2][k_{2\perp}^2+M^2(1-\eta_2)^2]}{\left[[k_{1\perp}^2+M^2(1-\eta_1)^2+\mu^2\eta_1]\{\eta_2(1-\eta_2)[k_{1\perp}^2+M^2(1-\eta_1)^2+\mu^2\eta_1]+(1-\eta_1)[k_{2\perp}^2+M^2(1-\eta_2)^2+\mu^2\eta_2]\}^2\right]}\quad(\eta_2=1-1/\eta_1 w),$$

$$\bar{F}_2^{(9d)}=(Z_{2(\pi^0)}-1)\bar{F}_2^{(9a)},$$

$$\bar{F}_2^{(9e)}=\left(\frac{g^2}{(2\pi)^3}\right)^2 4M\nu\int\frac{d^3P_2}{2E_2}\frac{d^3k_2}{2\omega_2}\delta(q^2-2k_1\cdot q)\left(\frac{\omega_1}{E_p}\right)^2\frac{4(M^2-P\cdot\bar{P}_1)(M^2+\bar{P}_1\cdot P_2)}{(2\bar{E}_1)^2(2\omega_1)^2(\bar{E}_1-E_2-\omega_1)^2(E_p+E_2-\omega_1+\omega_2)^2}$$

$$=2\left(\frac{g^2}{2(2\pi)^3}\right)^2\int d^2k_{1\perp}d^2k_{2\perp}\int_0^1 d\eta_2\frac{\eta_2^2(1-\eta_2)}{\{\eta_2(1-\eta_2)w[k_{1\perp}^2+M^2/w^2+\mu^2(1-1/w)]+k_{2\perp}^2+M^2(1-\eta_2)^2+\mu^2\eta_2\}^2}.$$

From these results and the similar ones in the Appendix of Paper II, we can now state how the substitution law (9) is satisfied among diagrams in the two channels, scattering and annihilation. For nucleon-current contributions, we have

$$F_2^{(17\alpha)}=\bar{F}_2^{(8\alpha)},\quad \alpha=\mathrm{a,b,c,d,e,f,g,h,i,j,k,l,o,p}$$

$$2F_2^{(17q)}+2F_2^{(17r)}+F_2^{(17g)}=\bar{F}_2^{(8g)}+\bar{F}_2^{(8q)},$$

$$F_2^{(17j)}=\bar{F}_2^{(8j_2)},$$

$$F_2^{(17m)}+F_2^{(17n)}=\bar{F}_2^{(8m)}+\bar{F}_2^{(8n)},$$

$$F_2^{(17s_1)}=\bar{F}_2^{(8r_1)}+\bar{F}_2^{(8j_3)},$$

$$F_2^{(17s_2)}+F_2^{(19t_2)}=\bar{F}_2^{(8s)},$$

$$F_2^{(17k_1)}=\bar{F}_2^{(8j_1)},$$

$$F_{2[n\pi^0]}=\bar{F}_2^{(8u)}{}_{[n\pi^0]},$$

where $F_{2[n\pi^0]}$ is given by (90) of Paper II. For pion-current contributions we give a few examples:

$$F_2^{(18\alpha)}=\bar{F}_2^{(9\alpha)},\quad \alpha=\mathrm{a,c,e}$$

$$F_2^{(18b)}+2F_2^{(18g)}+2F_2^{(18h)}=\bar{F}_2^{(9b)}+\bar{F}_2^{(9d)}.$$

To these results we add a few remarks: (i) The particular parametrizations accompanying each diagram make transparent the crossing properties once the transverse-momentum cutoffs in scattering and annihilation are identified. For this purpose, negative η's are sometimes used as in Figs. 8(a), 8(j), 9(a)–9(c), and 9(e), in accordance with the sign change in $(w-1)$. (ii) $\bar{F}_2^{(8r_1)}$, $\bar{F}_2^{(8r_2)}$, $\bar{F}_2^{(8t_2)}$, and $\bar{F}_2^{(8j_3)}$ separately diverge logarithmically at the end point $\eta_1'=0$. However, the sums $\bar{F}_2^{(8r_2)}+\bar{F}_2^{(8t_2)}$ and $\bar{F}_2^{(8r_1)}+\bar{F}_2^{(8j_3)}$ are well defined. (iii) For reasons already explained in Paper II, in Fig. 8(m) only the bubble in which both the proton and the pion have positive longitudinal momenta is included, and in Fig. 8(n) only $\delta M_a^{(1)}$ is retained. (iv) In old-fashioned perturbation theory because of, among other things, the time ordering in the vertices, there is no one-to-one correspondence between diagrams in one channel and diagrams in the crossed channel; as a result, crossing works generally between one group of diagrams in one channel and another group of diagrams in the crossed channel, instead of on a one-to-one basis; (v) All the diagrams calculated here do not have any singularity as $w\to 1$, and therefore these results support our smoothness assumption about the structure functions near $w\sim 1$.